K. J. Puite

Institute for Atomic Sciences in Agriculture, Wageningen

Thermoluminescent properties of manganese doped calcium fluoride

Applications in radiation dosimetry

1971 Centre for Agricultural Publishing and Documentation

Wageningen

ISBN 90 220 0342 6

De auteur promoveerde op 28 mei 1971 aan de Rijksuniversiteit te Groningen op een gelijkluidend proefschrift tot doctor in de wiskunde en natuurwetenschappen.

Abstract

Puite, K. J. (1971) Thermoluminescent properties of manganese doped calcium fluoride; applications in radiation dosimetry. Agric. Res. Repts (Versl. landbouwk. Onderz.) 761, ISBN 90 220 0342 6, pp. 6 + 78, tables 12, figs. 34, Eng. summary.
Also doctoral thesis, Groningen.

The thermoluminescent (TL) properties of CaF_2:Mn (3-4 mole %), prepared by Philips, the Netherlands, have been studied in order to realize to some extent two aspects of the research program of the Institute for Atomic Sciences in Agriculture at Wageningen, the Netherlands,

a. the assessment of a reliable dosimeter for routine use during biological experiments in the gamma facilities and the reactor of the Institute.

b. the study of the radiation induced phenomena in anorganic crystals, which would lead to a better understanding of these phenomena in macromolecules.

It was shown that UV exposure of already read out CaF_2 gave rise to a second reading. The TL sensitivity of CaF_2 for alpha particles and protons and for thermal and fast neutrons was investigated. Use was made of the $^{10}B(n,\alpha)^7Li$ and $^{14}N(n,p)^{14}C$ reactions occurring in boron and nitrogen containing liquids surrounding the powder.

Thermally stimulated exo-electron emission and TL measurements using CaF_2 samples doped with 0.1 mole % and 2 mole % Mn and undoped samples have led to the conclusion that both electron- and hole traps are present in the CaF_2:Mn; Y^{3+} and other trivalent rare earth ions, being the electron traps and Mn^{++} ions, being the hole traps.

Contents

Samenvatting

De thermoluminescentieverschijnselen in CaF_2-poeder, dat geactiveerd is met 3-4 % mangaan en waarvan de kristalletjes ca. 10-15 μm groot zijn, zijn onderzocht. Dit materiaal werd bereid bij Philips, Eindhoven, voor het meten van stralingsdoses.

Bij poeder bestraald met gammastraling werd één enkele thermoluminescentiepiek gevonden. Met een opwarmsnelheid die constant gehouden werd op 24°C per minuut lag deze piek bij 260°C. In werkelijkheid bestond deze piek uit meer, niet afzonderlijk waarneembare, pieken veroorzaakt door verschillende typen dosimetrievangplaatsen van electronen en/of van gaten in het materiaal. Gewoonlijk worden tijdens de opwarmcyclus al deze vangplaatsen geleegd. Werd reeds éénmaal afgelezen poeder echter blootgesteld aan UV licht dan bleek een tweede aflezing mogelijk. Blijkbaar worden de dosimetrievangplaatsen onder invloed van dit UV licht gevuld vanuit dieper gelegen vangplaatsen.

Metingen van thermisch gestimuleerde exo-electronenemissie en thermoluminescentie, waarbij CaF_2 geactiveerd met 0,1 % en 2 % mangaan en niet geactiveerde monsters werden gebruikt, hebben aangetoond dat zowel vangplaatsen van electronen als van gaten aanwezig zijn in het CaF_2:Mn (Philips), te weten: Y^{3+} centra en andere driewaardige zeldzame aarden als electronenvangplaatsen en Mn^{2+} centra als gatenvangplaatsen.

De thermoluminescentiegevoeligheid van CaF_2 voor alphadeeltjes en protonen vergeleken met die voor gammastraling werd onderzocht. Hierbij werd het CaF_2-poeder omgeven met borium- en stikstofhoudende vloeistoffen en vervolgens bestraald in een veld van thermische neutronen. De in de vloeistoffen optredende kernreacties ^{10}B (n,α) ^{7}Li en ^{14}N (n,p) ^{14}C leidden tot een extra thermoluminescentiesignaal in het CaF_2 door de vrijkomende alphadeeltjes en protonen. Bij poeder omgeven met alcohol en bestraald met snelle neutronen ontstond een extra signaal afkomstig van de terugstoot-protonen die in de alcohol werden geproduceerd. De grootte van het signaal van de genoemde deeltjes vergeleken met dat van gammastraling bedroeg 3, 5 en 11 % respectievelijk, op basis

van de geabsorbeerde dosis in de vloeistof.

De thermoluminescentiegevoeligheid voor thermische en snelle neutronen zelf werd eveneens onderzocht. Voor thermische neutronen werd een gevoeligheid van 0,07 rad per 10^{10} n/s.cm^2 gevonden, terwijl de 'gevoeligheid' voor snelle neutronen met een gemiddelde energie van 1,7 MeV -0,43 rad per 10^{10} n/s.cm^2 bleek te zijn. Voor een verklaring van deze negatieve waarde werd een model ontworpen waarin werd ondersteld dat de 'gevoeligheid' bestaat uit enerzijds een positieve component afkomstig van de bijdrage van de ionisaties en anderzijds een negatieve component veroorzaakt door de productie van diepe vangplaatsen.

Biologische moleculen geven vaak thermoluminescentie na bestraling bij vloeibare-stikstoftemperatuur. De eerste resultaten van de metingen aan het eiwit collageen zijn eveneens opgenomen in dit proefschrift. Reeds bij doses van 25 rad bleek een duidelijk thermoluminescentiesignaal aanwezig.

1 Introduction

1.1 Apologia

Thermoluminescent (TL) powders were introduced some twenty years ago by Daniels (1950) and are at present widely used to monitor radiation fields. Applications are reported in radiation dosimetry, personnel radiation monitoring, radiotherapy, space research and pottery dating (Fowler and Attix, 1966; Auxier et al., 1968).

At the author's laboratory, the Institute for Atomic Sciences in Agriculture at Wageningen, the TL system is used for routine dosimetry of biological experiments.

This thesis describes, within the framework of the study of the radiation induced physical phenomena in different materials (anorganic crystals, non-biological macromolecules e.g. PMMA, biological molecules and biological material), some aspects of the use and properties of powder and single crystals of calcium fluoride doped with manganese (CaF_2:Mn). The behaviour of this material in different radiation fields has resulted in a better insight in the mechanism of its thermoluminescence and has contributed to dosimetry applications. Other techniques such as optical absorption and exo-electron emission have given additional information.

A start has been made with the application of the described techniques to irradiated biological material in order to obtain information about the different energy pathways arising during the sequence of events starting from ionization and excitation and leading to the ultimate biological end-point.

1.2 Thermoluminescence

When in crystalline insulators, having a bandwidth of ~ 10 eV between the conduction band and the valence band, electron- or hole traps are present due to structural imperfections (vacancies, impurities

etc.) ionizing radiation can excite electrons and holes from the valence band into these traps (Figure 1) (Schulman, 1967). Depending upon the properties of the traps the charged carriers may remain captured at room temperature. The two important parameters of the traps are the trap depth E, being represented by the distance of the trapping level to the bottom of the conduction band (Figure 1), and the frequency factor s, related to the presence of lattice vibrations. If trapping occurs, the absorption of sufficiently energetic light quanta or an increase of lattice vibrations as the temperature is raised will cause ejection of the electrons or holes from their traps (Figure 1, step 1,1[1]). After migration through the conduction band, resp. valence band (step 2,2[1]) a recombination of an electron (resp. hole) with a trapped hole (resp. electron) can follow (step 3,3[1]). The recombination energy can be emitted in the form of a light quantum. When this luminescence is due to light absorption it is called 'optically stimulated luminescence'. In the case of a temperature increase the phenomenon is called 'thermo-

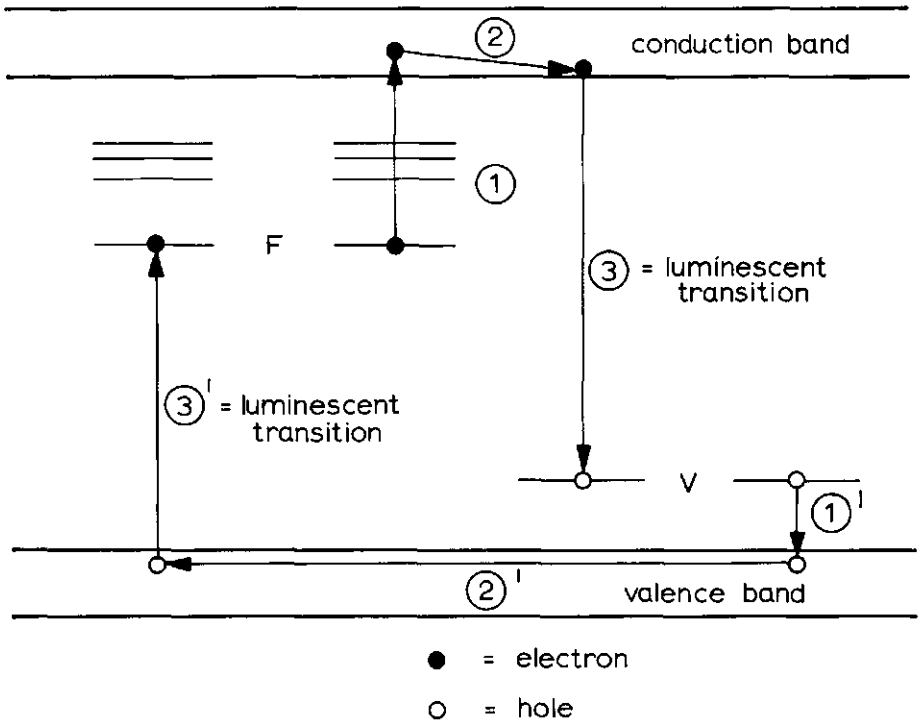

Fig.1. Schematic representation of thermoluminescence (Schulman, 1967). Two different types of centers are shown which may occur after irradiation, namely a F-center (an electron trapped at a negative ion vacancy) and a V-center (consisting of a trapped hole).

luminescence'.

The thermoluminescent process will be controlled by doping the material with specially chosen luminescent ions, e.g. Mn^{++} ions. In this case the hole is believed to be trapped after irradiation at these Mn^{++} ions (Schulman, 1967). After recombination of the electron and hole the luminescent ion will be in an excited state, emitting its characteristic luminescence (for Mn^{++} ions the green-orange region of the spectrum) when returning to the ground state.

The luminescent signal recorded as a function of a linearly increasing temperature is called a 'glow curve'. In the case of one kind of electron trap with a trap depth E and assuming no retrapping but a direct recombination with a hole resulting in a luminescent effect, Randall and Wilkins (1945) have derived the following mathematical expression for the thermoluminescent signal,

$$I\ (T) = n_o s \exp\ (-E/kT) \exp \int_{T_o}^{T} - \frac{s}{\beta} \exp\ (-E/kT)\ dT \qquad [1]$$

with I (T) = thermoluminescent signal

n_o = number of electrons initially trapped

s = frequency factor

E = trap depth

k = Boltzmann's constant, 8.61×10^{-5} eV/°K

β = heating rate

The temperature of the glow curve maximum T_m and the fading of the TL signal are both dependent on the values of E and s. Theoretical glow curves for different E and s values and a constant value of β are shown in Figure 2. T_m moves to higher temperature as E or β increases or as s decreases. The area under each curve is proportional to n_o, while in general n_o is proportional to the radiation absorbed dose. Traps having $E < 0.8$ eV along with $s > 10^9$ sec^{-1} do not store the electrons well at room temperature. The mean lifetime τ of electrons in these traps, expressed as

$$\tau = \frac{1}{s \exp\ (-E/kT)} \qquad [2]$$

is < 1 day (Schulman, 1967).

A list of prefered qualities for TL powders is given in (Schulman,

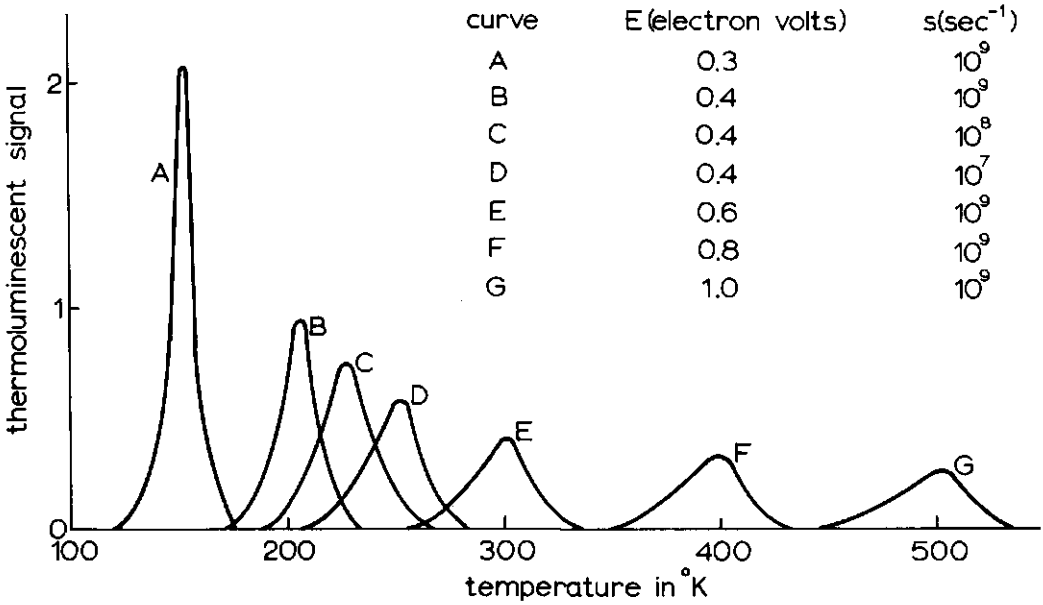

Fig.2. Theoretical glow curves for phosphors with a single trap depth and no retrapping, having a constant heating rate of 2.5°C/sec (Schulman, 1967).

1967). The properties of the most frequently used powders are dealt with in the following section.

For the temperature of the glow peak maximum T_m, at $dI/dT = 0$, it follows that

$$\beta E/kT_m^2 = s \exp(-E/kT_m) \qquad [3]$$

This equation makes it possible to calculate the value of both E and s, knowing the value of T_m at a certain heating rate β.

For $T < T_m$ the integral part given in equation 1 may be taken as a constant. Then

$$\ln I = -E/kT + \text{a constant term} \qquad [4]$$

and the E and s values may also be derived from the initial rise of the glow peak.

It should be born in mind that the luminescence efficiency L, defined as

$$L = \frac{P_r}{P_r + P_{nr}} \qquad [5]$$

where P_r and P_{nr} are the probabilities of luminescence emission and non-radiative emission, respectively, decreases with increasing temperature (Gorbics et al., 1969a), because P_r is assumed to be independent of temperature but P_{nr} increases with temperature. This 'thermal quenching' effect influences the thermoluminescent output and thus the T_m value of a glow peak.

1.3 Properties of thermoluminescent powders, especially CaF_2:Mn

Methods of preparing thermoluminescent CaF_2 powder doped with different manganese concentrations have been studied by Ginther and Kirk (1957) (Figure 3). Also CaF_2 doped with other activators such as Y, Sm, Ce, Eu and Yb has been studied (Görlich et al., 1961).

The glow curve of CaF_2:Mn (3 mole % Mn) has only one apparent maximum at about 260°C. The emission spectrum has its maximum at 500 nm. This glow curve consists of several components (Schulman et al., 1969). When rapid heating rates (~ 20°C/sec) are applied the glow curve components shift to higher temperature, causing preferential quenching of the more stable higher components. This results in a fading of

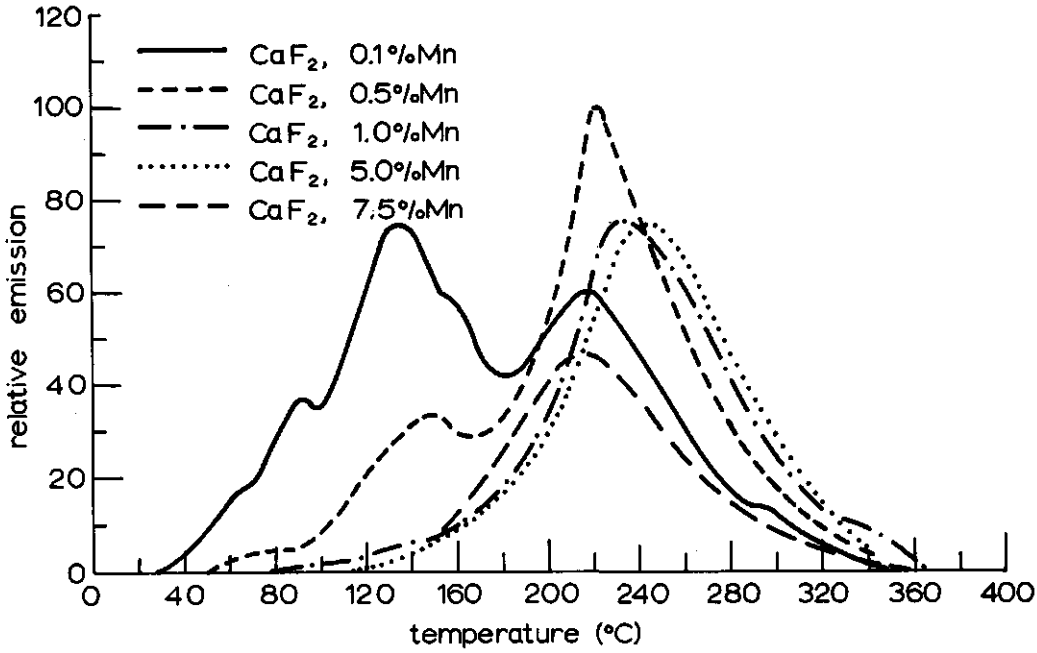

Fig.3. Thermoluminescence of synthetic CaF_2:Mn as a function of the Mn content in mole % (Ginther and Kirk, 1957).

~ 10 percent during the first month. Fading is negligible if a slow heating rate is used (~ 20°C/min).

From the measured shift in glow peak temperature vs. heating rate Gorbics et al. (1969b) calculated values for E and s, using equation 3, namely E = 2.29 eV and s = 2.5 x 10^{19} sec^{-1}. No simple interpretation of these values is possible because of the complexity of the material compared to the single trap model which has been assumed by Randall and Wilkins (1945).

In Figure 4 the TL response of CaF_2:Mn (3 mole % Mn) as a function of ^{60}Co gamma ray exposure is shown, together with the responses of other common TL powders (Marrone and Attix, 1964; Cristensen, 1968). For CaF_2 a linear response up to 2 x 10^5 R is obtained. LiF and $Li_2B_4O_7$:Mn (0.1 % by weight of Mn) exhibit 'supralinearity' for exposures exceeding 300 R. When low energy X rays are used, the CaF_2 dosimeters have a considerable energy dependence, as shown in Figure 5 (Almond et al., 1968).

During the last years an extensive literature has appeared dealing with thermoluminescent dosimetry (Lin and Cameron, 1968; Spurny, 1969).

1.4 Thermally stimulated exo-electron emission, especially of CaF_2

Electrons released from their traps into the conduction band will, in general, give rise to three types of effects which may be observed simultaneously, namely,

a. electrical conductivity of the crystal, proportional to the electron concentration in the conduction band (conductivity glow curve) (Kanturek, 1956).

b. electron transfer to activator levels resulting in photon emission (TL glow curve).

c. electrons leaving the surface with a probability dependent on temperature and work function (exo-electron emission). The work function φ is defined as the minimum energy needed for an electron located at the bottom of the conduction band to escape from the crystal surface. Figure 6 gives an illustration of these processes.

Besides the TL phenomena mentioned in section 1.2, also thermally stimulated exo-electron emission (TSEE) has been studied because TSEE data may give additional information about the electron traps.

The interpretation of the experimental data sometimes leads to

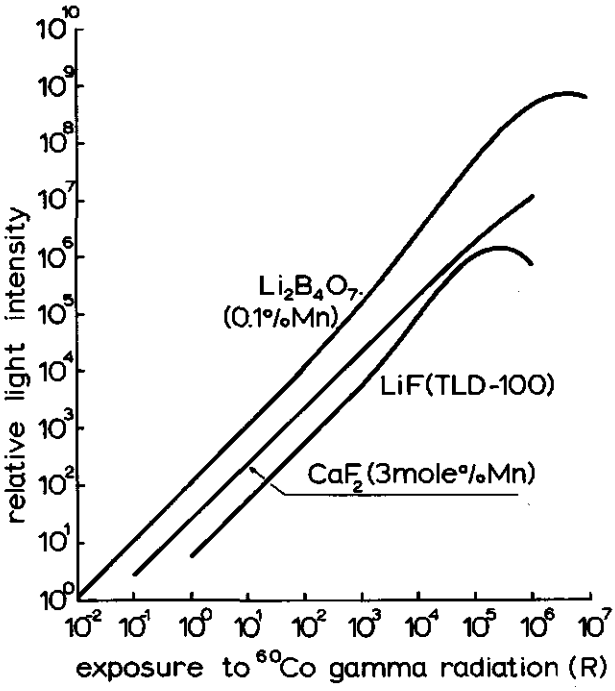

Fig.4. Thermoluminescent response of CaF_2:Mn (3 mole %), LiF and $Li_2B_4O_7$:Mn (0.1 % by weight of Mn) to ^{60}Co gamma rays (Marrone and Attix, 1964; Cristensen, 1968).

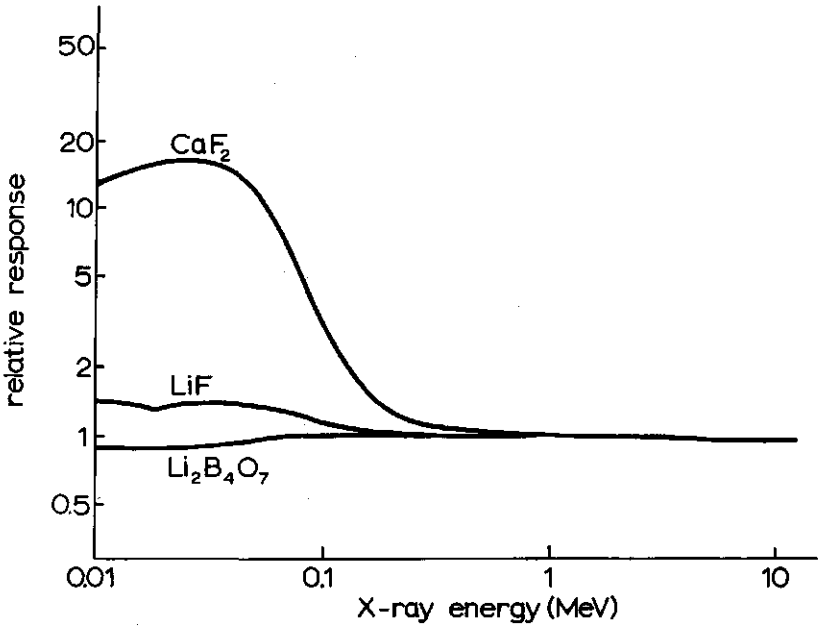

Fig.5. Calculated relative response of CaF_2, LiF and $Li_2B_4O_7$ versus energy (Almond et al., 1968).

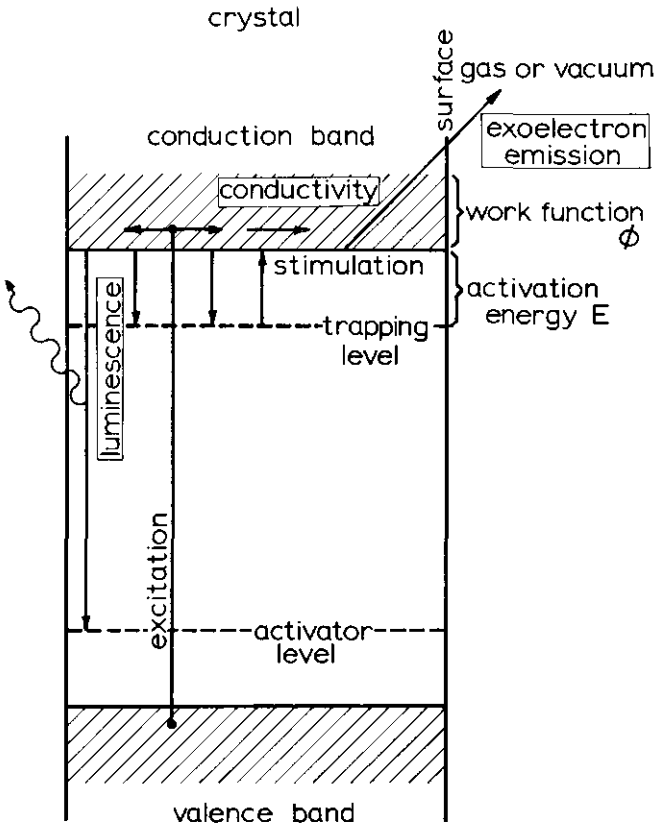

Fig.6. Diagram of the relation between luminescence, conductivity and exo-electron emission during thermal or optical stimulation of an ionic crystal which has been exposed to ionizing radiation (Becker, 1970).

difficulties, because the kinetics of TSEE are not yet completely understood. Two processes are assumed to be involved,

a. an emission from the traps via the conduction band.

b. a direct emission from the traps at or near the surface.

A distinction should in fact be made between surface traps and traps in deeper layers of the crystals (volume traps). Electrons from the volume traps reach the conduction band after thermal stimulation and obtain a Maxwellian distribution. After overcoming the work function φ part of the electrons leave the crystal surface with an average energy of sore 0.1 eV. The emitted electrons originate from a thin surface layer of 10 - 100 Å (Kramer, 1967; Holzapfel, 1969). The influence of the thickness of the emitting layer is small as long as the distance of location of the exo-electron emission from the surface

is comparable with the free path length of the electrons. Values of the work function φ up to 1 eV do not affect the TSEE much at room temperature (Holzapfel, 1969) (Figure 7).

Although TSEE can be considered as a non-stationary thermionic emission because of the limited supply of electrons from the traps, Holzapfel (1969) has derived some mathematical expressions for TSEE based on the Richardson equation for stationary thermionic emission,

$$\frac{dn_{ex}}{dT} = \frac{n_c}{\beta} \left(\frac{kT}{2\pi m_{eff}}\right)^{1/2} \exp\left(-\varphi/kT\right) \qquad [6]$$

with n_{ex} = number of electrons emitted per unit surface

n_c = number of electrons instantaneously present in the conduction band per unit volume

β = heating rate

m_{eff} = effective mass of electron

φ = work function

Assuming no retrapping, equation 6 leads to

$$\beta E/kT_m^2 = s \exp\left(-(E + \varphi)/kT_m\right) \qquad [7]$$

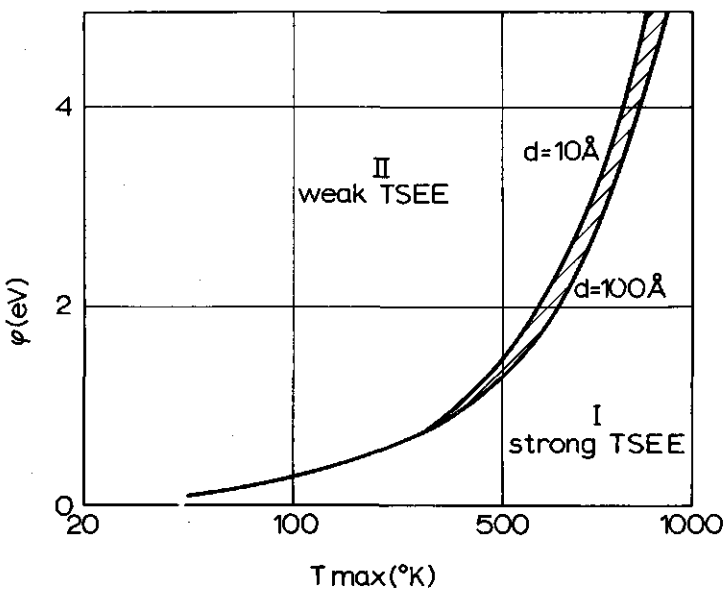

Fig.7. Calculated areas of weak and strong TSEE for different work functions φ, peak temperatures T_m and emission layers d (Holzapfel, 1969).

in the area of weak TSEE (see Figure 7), giving the relation between the trap depth E, the work function φ and the peak temperature T_m. For $\varphi = 0$ equation 7 gives the mentioned relation in the area of strong TSEE.

When the distance of location of the exo-electron emission from the surface is much longer than the free path length of the electrons, diffusion of electrons from these deeper layers to the surface has to be taken into account. Exact calculations become then much more complicated.

The first systematic studies on exo-electron emission were published by Kramer (1949). Review articles appeared from Bohun (1963) and from Becker (1970). The 1970 review describes the possibilities for TSEE dosimetry.

CaF_2, in particular, has been studied by Kramer (1951), Bohun (1955) and Dolejsi et al. (1958). In 'chemically pure' CaF_2 three TSEE maxima were observed at 80°, 165° and 240°C, corresponding to trap depths of 0.71, 0.91 and 1.03 eV, respectively (Sujak and Gieroszynska, 1967).

1.5 Color centers in CaF_2

When radiation induced trapped electrons or holes, which are normally in the ground state (see Figure 1), absorb light quanta of the proper energy, transitions to higher excited states are possible. Absorption of light in the visible region of the light spectrum results in a coloration of the crystal. The imperfections causing light absorption are called color centers.

This section describes some relevant color centers in CaF_2. The structure of these crystals can be regarded as a regular cubic array of fluorine ions with calcium ions at every other body center. Thus each calcium ion is at the center of a cube of eight fluorine ions.

Coloration by irradiation of commercially available CaF_2, often called subtractive coloration, only occurs at room temperature when high doses are used of at least 10^5 rad. Results of O'Conner and Chen (1963) suggest that this coloration is due to the reduction of trace impurities of Y^{3+}, which has the same ionic radius (1.06 Å) as Ca^{++}. The spectrum (Smakula type) consists of four band at 225, 335, 400 and 580 nm. Doses exceeding 5×10^6 rad cause additional absorption bands

in the infrared region, probably due to the formation of rather complex defect centers (Fong and Yocom, 1964). In addition, oxygen is often found as an impurity in CaF_2 (Fong and Yocom, 1964). If an O^{--} ion is substituted for a F^- ion, electrical neutrality requires that either a F^- ion vacancy or a trivalent positive ion such as Y^{3+} is present.

For very pure CaF_2, irradiation and optical measurements must take place at liquid nitrogen temperature or lower in order to produce any coloration (Kamikawa et al., 1966; Görlich et al., 1968). The absorption band observed at 375 nm was ascribed to F-center absorption based on the identification of the data already obtained with additively colored CaF_2. Additively colored crystals show an absorption band at 375 and 520 nm (Mollwo type). The 375 nm band has been correlated with F-centers by Arends (1964). The 520 nm band is probably due to M-centers (den Hartog, 1969).

In CaF_2 doped with manganese, radiation induced complex color centers may be expected when trace impurities such as yttrium and oxygen are also present. The Mn^{++} ions are probably situated at Ca^{++} ion lattice positions. Electron spin resonance (ESR) experiments on CaF_2 doped with 0.01 mole % Mn have given patterns which were in close agreement with the calculated ones assuming that the Mn^{++} ion is substituted for the Ca^{++} ion. A fluorine hyperfine structure due to the covalent bonding between the Mn^{++} ion and the surrounding fluorine ions was observed (Baker et al., 1958).

1.6 Thermoluminescence of biological material

The interaction of ionizing radiation with solid biological material e.g. nucleic acids, amino acids, proteins starts with excitation and ionization events (Hart and Platzman, 1956) and may ultimately result in observable damage in the material. During this sequence of events light emission may occur.

A model which describes especially those processes which are of importance for the observed luminescent phenomena is shown in Figure 8 (McGlynn et al., 1964; Steen, 1968). The configuration of the molecular orbital electrons which best describes the ground state and the lower excited levels of the molecule is represented by the boxes beside each energy level. Also the spin of the highest energy orbital electrons is given. Depending on the relative direction of the spins singlet and

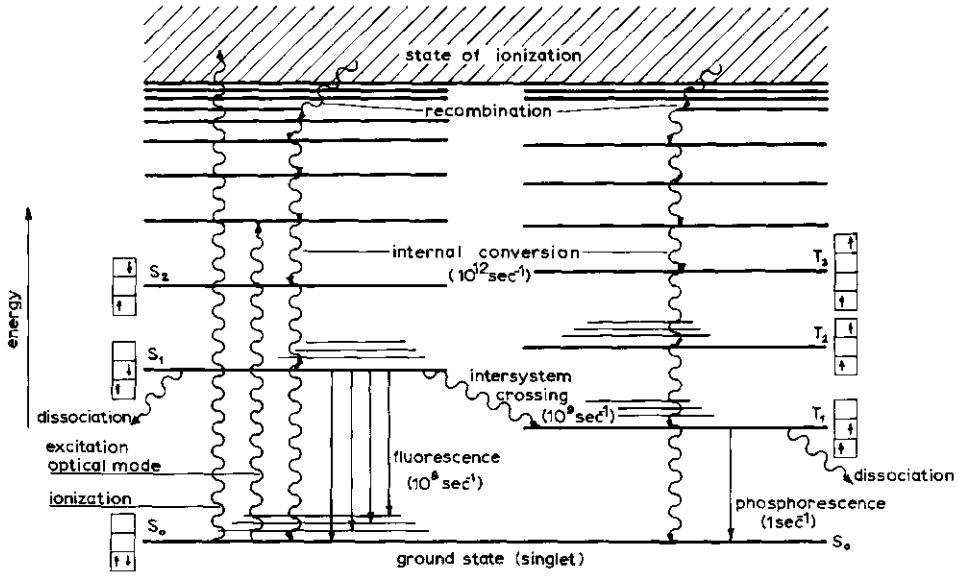

Fig.8. Energy level diagram for organic molecules (McGlynn et al., 1964; Steen, 1968).

triplet levels arise.

After ionization the electrons will escape from their parent ions and will move some Å away from their origin before being thermalized. During this process the electrons may be trapped in the material by polarization of neighbouring molecules. These trap depths are of the order of ~ 0.1 eV, the traps being stable only at low temperatures (below 100°K). When the material is heated, the electrons are released from their traps and may recombine with the positive ions. This recombination leads to excitation of singlet and triplet states. These states decay via internal conversion to the lowest excited states S_1 and T_1, dissipating the excess energy as vibrational energy to the surrounding molecules. Also rupture (biological damage) of the molecules may occur during this process. From the lowest excited singlet level S_1 (life time ~ 10^{-8} sec) transitions are possible to the ground state S_o and also via intersystem crossing to the lowest excited triplet state T_1. The $S_1 \rightarrow S_o$ transitions result in fluorescence emission in competition with non-radiative transitions. Phosphorescence emission is possible when the lowest excited triplet level T_1 (~ 1 sec) is de-excited. This $T_1 \rightarrow S_o$ transition is also in competition with non-radiative processes.

Thus, on heating the material both fluorescent and phosphorescent

biochemical	R group of general structure R-CH(NH_2)-COOH	T_m(°K) β=12°K/min	trap depth (eV) from initial rise	ref	intensity	ref
<u>amino acids</u> L-tyrosine	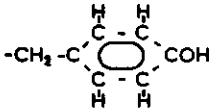	112 151	0.16 0.25	40	10000	36
L-tryptophan	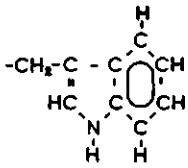	105 133 177	0.19 0.25 0.39	40	2850 1830	36
L-phenylalanine	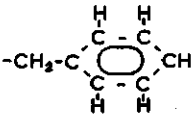	118 133 174	0.22 0.29 0.31	40	430 240	36
L-alanine	$-CH_3$	143 165	0.04 —	36	0.8 0.4	36
glycine	-H	133 167 236	— 0.23 —	36	0.3 0.7 0.2	36
proline	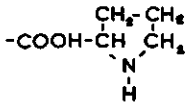	147 166 240	0.05 — 0.21	36	6 5 2	36
L-hydroxy-proline	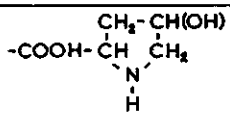	115 ~145		39	60 50	39
<u>proteins</u> trypsin		122	0.09	40	60	36
gelatin		111	0.05	36	30	36

Table 1. Data on the thermoluminescence of some biochemicals irradiated with ^{60}Co gamma rays (Augenstine et al., 1960; Augenstine et al., 1961; Weinberg et al., 1962).

emission may occur and will be recorded as thermoluminescent emission of the material.

Various low-temperature thermoluminescence studies on biological molecules have been reported from about 1960 (Augenstine et al., 1960; Singh and Charlesby, 1965; Fleming and Kerr, 1965) (see Table 1).

The intensity of the TL from amino acids having a ring structure is about two or three orders of magnitude greater than the intensity from the aliphatic amino acids (Augenstine et al., 1960). Most of the glow peaks lie between 100° and $170^{o}K$. Augenstine et al. (1961) observed that the TL from irradiated proteins is not the sum of the independent contributions from the constituent amino acids, whilst the trap depths E for the TL of proteins were much smaller than those obtained for the constituent amino acids. Emission spectra of the TL of trypsin did not resemble any of the spectra observed for the aromatic amino acids (Weinberg et al., 1962). Lehman and Wallace (1964) have listed TL data of a large number of biologically important molecules using radiation sources with different linear energy transfer. Nummedal and Steen (1969) observed that the majority of the species giving rise to TL of the protein studied were trapped intramolecularly or at least within a distance of 20 Å of the emitting molecules. The $T_1 \rightarrow S_o$ transition was found to be the only radiative step. Also complex biochemicals were studied. A possible correlation between TL and radiosensitivity of seeds was demonstrated by Cervigni et al. (1969).

2 Materials and Methods

2.1 Materials

2.1.1 CaF_2:Mn powder

The CaF_2:Mn powder used in this work was prepared at the Philips laboratories, Eindhoven. A mixture of calcium fluoride and manganese fluoride powder was heated in a nitrogen atmosphere and after cooling was milled and sieved through a B 40 silk gauze[1]. Grain sizes of 10 - 15 μm were obtained. The manganese content was determined at ITAL by neutron activation analysis[2]. For the two batches used, and indicated as # 4 and # 5, a concentration was found of 4.1 and 3.4 mole %, respectively. Batch # 5 is used only in the experiments described in section 3.5 of this thesis. Röntgenfluorescence measurements, carried out at the Laboratory for Solid State Physics, Groningen[3] showed the presence of strontium in the samples. As was revealed in the results of the experiments yttrium is also present. The Y^{3+} concentration, being 0.03 ppm, was measured at the Philips laboratories[4] by neutron activation analysis. Apart from yttrium, also the presence of other impurities could be demonstrated. The data are collected in Table 2 of

1. The relevant information obtained from Dr. K. Nienhuis and Mr. Th.C. Alferink of the Philips laboratories is gratefully acknowledged.

2. This analysis was kindly performed by Mr. N. van der Klugt.

3. The author is indebted to Prof.Dr. J. Arends and Mr. F. van der Horst for performing these measurements.

4. The yttrium analysis was kindly carried out by Mr. P. Bruys.

section 2.1.2.

2.1.2 Other CaF_2 samples

Other CaF_2 samples have also been used,

a. CaF_2 crystals from Materials Research Corporation [5] (MRC). Strontium and yttrium (7.6 ppm) impurities were present in the crystals.

b. CaF_2 from MRC doped with ~ 2 mole % Mn. Also strontium and yttrium impurities were present.

c. CaF_2 crystals doped with 0.1 mole % Mn from Semi-Elements [6]. The

	Philips	MRC	Semi-El.	Harshaw
Y	0.03	7.6	8.3	0.17
Lu	≦0.006	0.07	0.08	0.006
Yb	≦0.02	0.3	0.4	0.02
Tm	≦0.2	≦0.2	≦0.2	≦0.2
Ho	≦0.3	0.4	0.3	≦0.3
Tb	≦0.002	0.04	0.04	0.002
Eu	0.009	0.2	0.04	0.006
Sm	≦0.2	0.2	0.2	≦0.2
La	0.03	0.1	0.1	0.1
Nd	≦0.1	≦0.1	≦0.1	≦0.1
Ce	≦0.1	≦0.1	≦0.1	≦0.1
Au	0.002	0.002	0.002	0.005
Cd	≦1	1.5	1	≦1
Sr	200	70	70	250
Sb	0.3	0.05	0.15	0.04

Table 2. Impurities (ppm) in CaF_2 samples as measured at the Philips laboratories, the Netherlands.

5. *Materials Research Corporation, Orangeburg, New York 10962, U.S.A.*

6. Semi-Elements, Inc. Saxonburg, Pa. 16056, U.S.A.

yttrium contamination was 8.3 ppm.

d. CaF_2 from the Harshaw Co[7]. These were pure crystals with 0.17 ppm of yttrium.

e. CaF_2 from Vinor[8]. These crystals were very pure and free of yttrium. Oxygen seemed to be the only impurity present.

The impurities which could be demonstrated by neutron activation analysis are collected in Table 2.

2.1.3 Collagen

Collagen has been chosen as a starting material to study the TL of biological tissues for the following reasons,

a. the biochemistry of collagen is rather well known (Veis, 1964; Bailey, 1968a).

b. the structure of the collagen molecule is thoroughly investigated (Harrington and von Hippel, 1961).

c. collagen comprises about 30 % of the total organic matter in mammals.

d. electron spin resonance (ten Bosch, 1967) and other techniques such as optical rotation and viscosity measurements (Welling and Bakerman, 1964; Bailey, 1968b) have been used to investigate radiation effects on collagen.

The fundamental molecular unit of all collagens is thought to be a tropocollagen molecule 15 Å in diameter and 2800 Å long, having a molecular weight of about 3×10^5. The structure of tropocollagen has been investigated by Rich and Crick (1961) and by Ramachandran (1963) and was found to be a triple-helix with hydrogen bonding between the three single chain helices. The amino acid sequence of one helix seems to be Gly-Pro-Hypro, Gly-X-Hypro and Gly-X-Pro, with X being any amino acid present. For further details about collagen see (Veis, 1964; Bailey, 1968a).

The collagen used in the preliminary experiments described in section 3.6 was extracted from bovine Achilles tendon and was purchased

7. The Harshaw Chemical Co., Cleveland 6, Ohio, U.S.A.

8. Vinor Laboratories, Medford, Mass. 02155, U.S.A.

from the Koch-Light laboratories [9].

2.2 Instrumentation

2.2.1 Thermoluminescence

The apparatus used for most of the thermoluminescence measurements was a modified, commercially available, CONRAD Model 4100 TLD reader [10]. 45.0 mg of the CaF_2 powder was weighed onto a planchet and heated by passing an electric current through the planchet. The cycle time of the apparatus was such that the planchet was heated to 370°C at a rate of 2.7°C/sec. The TL of the powder was detected with a photomultiplier. A clear pyrex glass dish served as electrical and thermal insulator for the photo-kathode. For integral readings the photomultiplier signal was fed into a Solartron digital voltmeter, type LM 1420. A constant light source, consisting of a ^{14}C activated scintillator, was used for calibration of the instrument.

In the experiments mentioned in section 3.5 the TL signal was measured with a specially constructed apparatus allowing a slow and strictly linear heating rate of the powder at a rate of 24°C/min.

2.2.2 Thermally stimulated exo-electron emission

The TSEE experiments were made using a cylindrical gas flow counter with a diameter of 90 mm and a height of 30 mm, which was specially constructed for the purpose. The position of the furnace is shown in Figure 9. The CaF_2 powder was heated in three 1 mm deep holes which each have a diameter of 0.9 mm. A chromel-alumel thermocouple, situated at a distance of 3 mm from the holes, served as a reference in order to obtain a constant heating rate of 24°C/min at the position of the powder. The temperature at this position and the influence of the gas flow on the temperature was determined with a copper-constantan

9. Koch-Light laboratories Ltd., Colnbrook, England.

10. Controls for Radiation, Cambridge 40, Massachusetts, U.S.A.

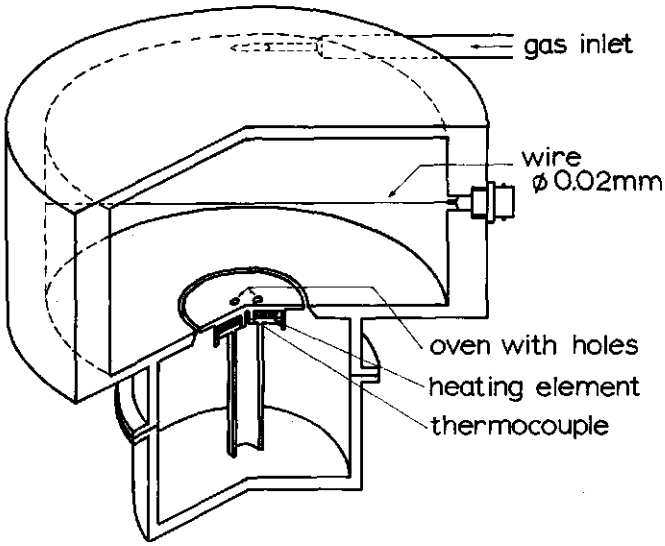

Fig.9. Apparatus for measuring the TSEE signal.

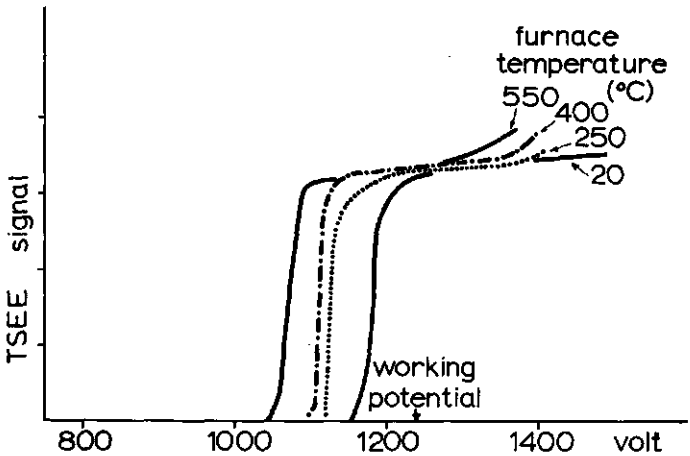

Fig.10. GM plateau's obtained with the TSEE apparatus for different furnace temperatures.

thermocouple situated in one of the holes, filled with CaF_2 powder. Thin thermocouple wires (diameter 0.13 mm) were used to avoid heat leakage as much as possible. The temperature difference between the positions of the thermocouples was 15°C at 250°C both with and without gas flow. The estimated error in the temperature measurement of the TSEE peaks is ± 5°C. A mixture of helium gas (98.7 %) and isobutane (1.3 %) was used as counting gas. This gas mixture was injected tangentially into the counter and flowed through the counter at a constant rate during the measurements. A useful GM plateau could be obtained up to a

furnace temperature of 500°C (Figure 10). The GM signal recorded using a small external ^{60}Co source increased approximately 1%/100°C when the furnace was heated from 20° to 500°C.

2.2.3 Optical absorption

A double beam Unicam SP 700 recording spectrophotometer (range 187 nm - 3.57 μm) was used for the optical absorption measurements. All the measurements were carried out at room temperature.

2.3 Irradiation facilities

2.3.1 Gamma sources

Two gamma facilities were available for the experiments, a 300 Ci and a 5000 Ci ^{137}Cs source (E_γ = 0.66 MeV, $T_{1/2}$= 30 y). An irradiation position close to the source pipe of the 5000 Ci source permitted irradiations with dose rates of 5-30 krad/h. A turn table was used to ensure a homogeneous irradiation. The calibration of this source was carried out with the Fricke ferrous sulphate dosimeter, which is a secondary standard chemical dosimeter (Holm et al., 1961; Law, 1970). The Fricke dosimeter has a working range of 4-40 krad and consequently could not be used to measure the dose rate of the 300 Ci source directly. LiF dosimeters and ionization chambers, calibrated against the Fricke dosimeter, have been used in the radiation field of this source. A dose rate of 51.0 ± 0.6 krad/h was measured in July 1970 at a distance of 1 m from the source (Gouverneur and Puite, 1970).

2.3.2 BARN reactor

The neutron experiments have been carried out in the irradiation room of the 100 kW BARN reactor (Figure 11). The reactor is a light water moderated swimming pool type, utilizing enriched ^{235}U fuel. The irradiation room is situated under the reactor core and is separated from it by a D_2O filled diffusor 125 cm deep. Directly under the diffusor two bismuth shields (17.5 cm thickness totally) are present (Bogaardt et al., 1964).

The thermal neutron flux density in the room amounted to (0.5 -

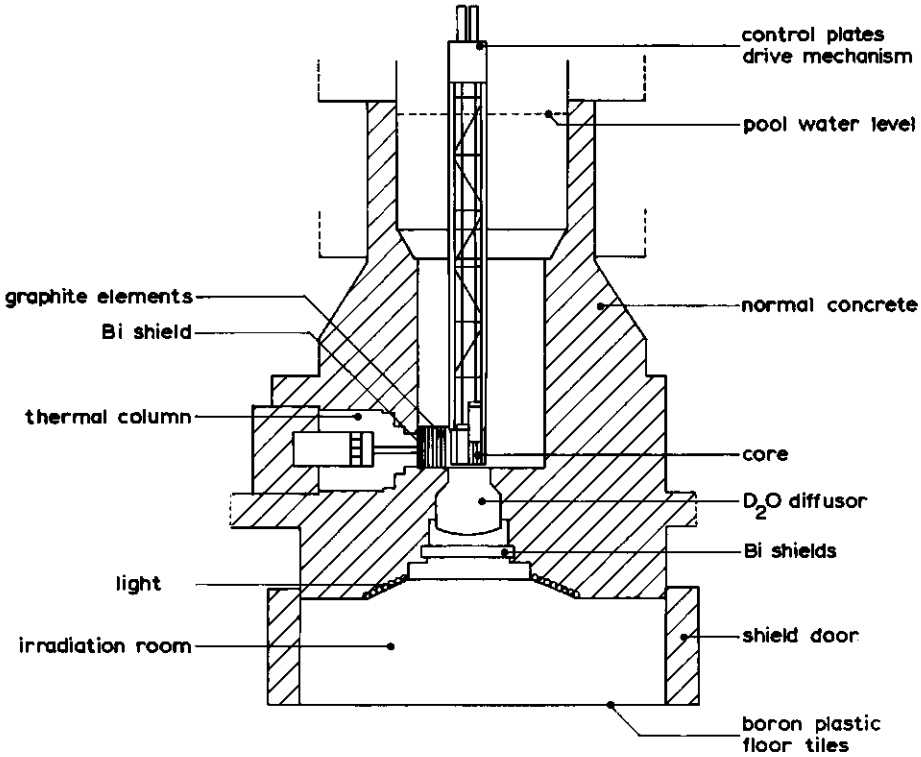

Fig.11. Vertical cross section of the BARN reactor.

4.5) x 10^7 n/s.cm^2 and was measured by gold foil activation. The cadmium ratio for gold was 300-500, indicating a low epithermal and fast neutron contamination of the thermal neutron beam. The gamma contamination, mainly from the H(n,γ)D reactions and from the reactor core, amounted to 2-9 rad/h and was measured using a teflon-CO_2 or a Mg-CO_2 ionization chamber (IAEA, 1967).

Fast neutron irradiations could be carried out by emptying the D_2O diffusor. To remove any thermal neutron contamination of the fast neutron beam a boron shield was inserted between the two bismuth gamma shields. Fast neutron spectroscopy and dosimetry in the irradiation room have been carried out using semiconductor sandwich detectors and tissue equivalent ionization chambers (IAEA, 1967; Chadwick and Oosterheert, 1969). The energy spectrum of the fast neutrons is shown in Figure 12 and is compared with a fission spectrum. The fast neutron dose rate in the room varied between 1-7.8 krad/h in H_2O, being equivalent to a flux density of (1-7.5) x 10^8 n/s.cm^2, with a gamma contamination of 80-300 rad/h. This gamma dose was measured with a Mg-A ionization chamber. The

chamber was assumed to be insensitive to fast neutrons (IAEA, 1967).

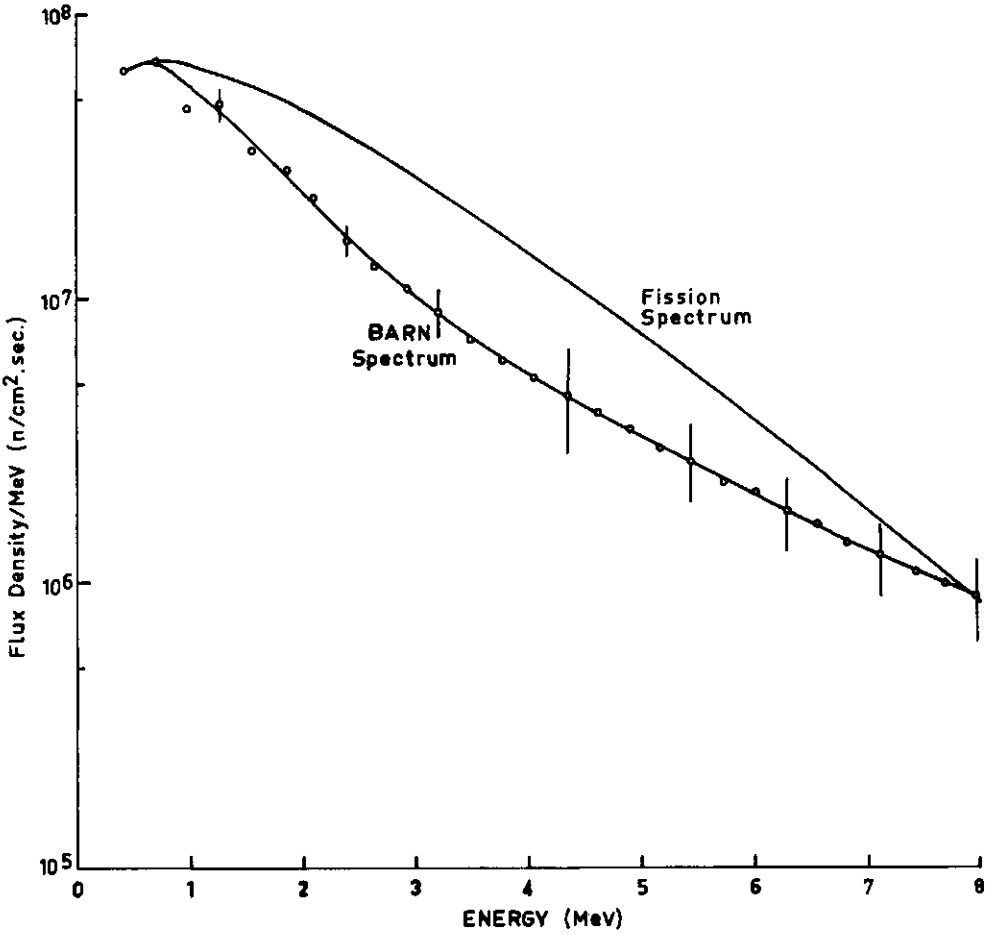

Fig.12. Comparison of the fission spectrum and BARN spectrum (normalized at 700 keV) (Chadwick and Oosterheert, 1969).

3 Experiments and Results

Two aspects of the ITAL research program could be realized to some extent by studying the effect of radiation of thermoluminescent CaF_2:Mn powder,

a. the assessment of a reliable dosimeter for routine use during biological experiments in the gamma facilities and in the BARN reactor.

b. the study of the radiation induced phenomena in anorganic crystals, which would lead to a better understanding of these phenomena and a better analysis of results obtained with macromolecules.

Consequently, these experiments have both a practical and a fundamental character. Firstly, some general properties of CaF_2:Mn have been investigated. In general, TL powder permits only one reading but with CaF_2:Mn repeated readings could be obtained. The possible use of CaF_2:Mn in measuring the gamma contamination of the thermal and fast neutron fields in the reactor was investigated and because of this the radiation parameters of these fields have been measured first. The TL response of CaF_2:Mn to alpha particles, protons and to thermal and fast neutrons are described in the following sections. Additional techniques such as TSEE and OD (optical density) measurements have been applied to obtain information about the trapping centers in CaF_2:Mn.

3.1 General features of thermoluminescent CaF_2:Mn

The CaF_2:Mn powder used has the following general properties,

a. a single glow peak with a T_{max} at 260 $\pm$ 3°C is recorded when gamma irradiated powder is heated at a strictly linear rate of 24°C/min (see section 3.5.1).

b. from the initial rise of the glow curve the E and s values have been calculated using the equations 3 and 4 of section 1.2. The values obtained were E = 1.05 eV and s = 1.5 x 10^8 sec^{-1}. These values differ considerably from the values E = 2.29 eV and s = 2.5 x 10^{19} sec^{-1} mentioned by Gorbics et al. (1969b). Their calculation was based on the

observed shift of the glow peak maximum of CaF_2:Mn developed at the Naval Research Laboratory (Ginther and Kirk, 1956), when this powder was heated at different heating rates. In both cases no simple interpretation of the E and s values is possible because of the complexity of the glow peak compared to the single trap model assumed in the calculations.

c. after being 'read out', the powder can be re-used without any annealing procedure. No change in gamma ray sensitivity has been observed.

d. the fading of the TL response depends on the heating rate of the powder (Schulman et al., 1969). Readings have been carried out 24 h after irradiation using a moderate heating rate of 2.7°C/sec. This procedure guarantees a negligible fading of the TL signal.

e. each batch of CaF_2 may have a different gamma ray sensitivity making a new calibration necessary. Also powder from one batch which has been stored under different conditions (e.g. humidity) should be recalibrated.

3.2 Repeated thermoluminescent readings of CaF_2:Mn

published before as 'The effect of UV exposure on thermoluminescent CaF_2:Mn' in the International Journal of Applied Radiation and Isotopes, 1968, vol. 19, pp 397-402.

Introduction

During irradiation of thermoluminescent powder -e.g. CaF_2:Mn- electrons are ejected from the valence band into the conduction band. Vacancies and other crystal imperfections can act as trapping centers for those electrons. These traps are situated just beneath the conduction band. Especially when the traps are deep they generally store the electrons very well. A heat treatment can liberate the electrons from the traps. Via the conduction band they combine with a hole at a Mn^{2+} ion site resulting in an excited state of this ion. The emitted light is measured as the thermoluminescent (TL) response (Schulman, 1967). This response as a function of the temperature (glow curve) gives peaks at a temperature corresponding to the depth of the trap.

In an attempt to get more information about the mechanism of thermoluminescence, the influence of UV light on CaF_2:Mn has been

studied.

After the first read out of the irradiated powder no TL response is obtained when the powder is heated for a second time. Apparently the traps concerned are completely emptied by the first heat treatment. However, when the powder is exposed to UV light after the first read out a second TL response is found afterwards.

Some experiments have been carried out to find a relationship between the previous reading and the UV induced TL signal, the sort of trapping centers which are involved in the UV transfer process and the possibility of repeated readings with UV exposure.

Methods

The CaF_2:Mn used in the experiments was obtained from Philips (the Netherlands). This powder is less sensitive (Schayes et al., 1967) than that prepared at the U.S. Naval Research Laboratory (Ginther and Kirk, 1956) and its response is linear for gamma rays up to 2 x 10^5 rad. The glow curve exhibits a single peak at the same temperature (260°C) as the NRL powder.

After the normal read out of irradiated powder and controls (heating rate 2.7°C/sec) the filled planchets were placed on a turning table and subjected to UV from a Philips HPLR mercury lamp. The energy flux of the UV measured through a Schott UG 5 2 mm filter was 26 W/m^2 at the position of the planchets. The variation of the light intensity amounted to about 1 % during the experiments. After the UV treatment the powder was read out again. Only the previously irradiated CaF_2:Mn gave a TL response.

For a gamma dose range of 0.2-50 krad the transferred TL was measured after a 35 min UV exposure corresponding to 5.5 W.sec/cm^2. The heating cycle was switched off at about 460°C because of the infrared interference.

Results

The results are shown in Figure 13. From 0.2-5 krad the response was 3.5 % of the original response. From 10-50 krad the percentage amounted to 5 %. Alpha (2.9-4.1 krad) and proton (0.7-2.0 krad) irradiations gave values of 5 and 9 % respectively.

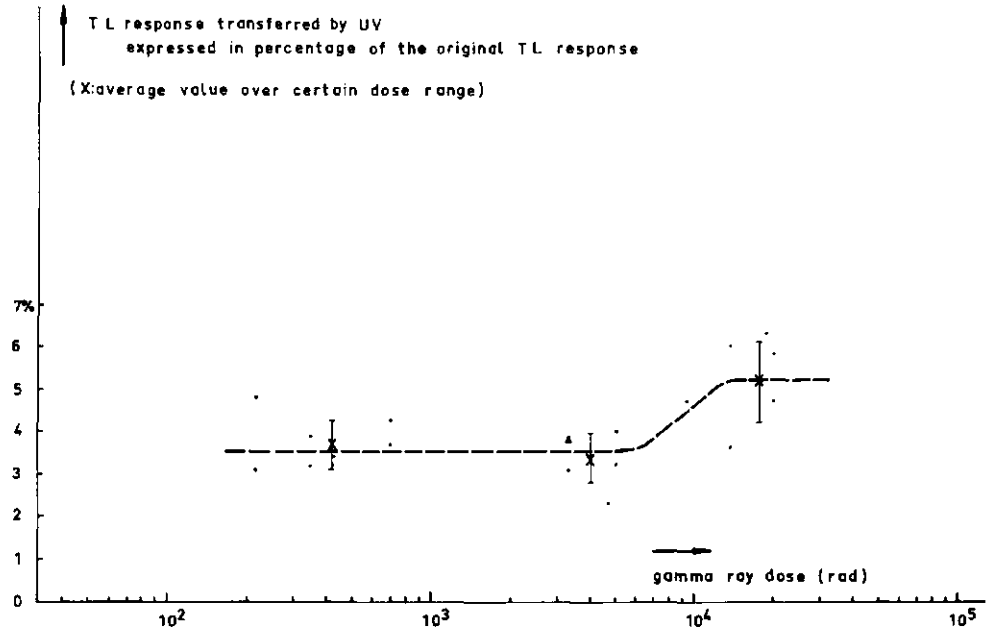

Fig.13. The increase of the TL response transferred by UV exposure starting at 10 krad.

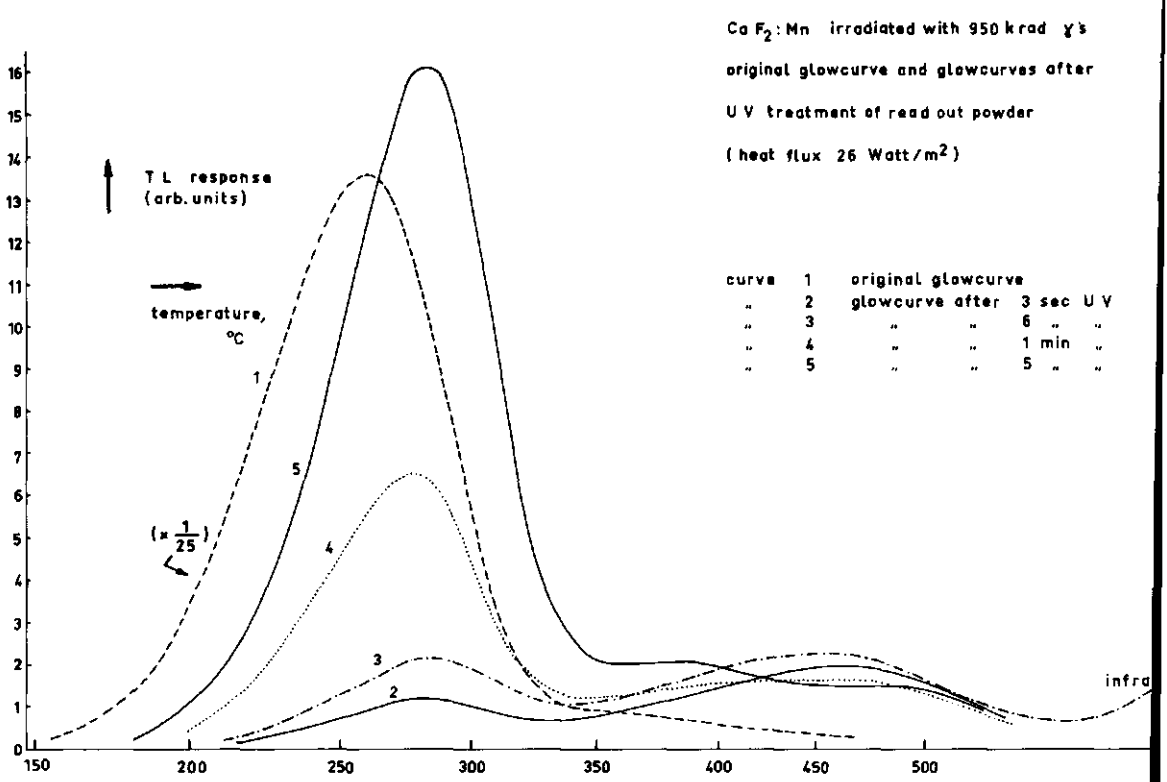

Fig.14. Original glow curve and glow curves of CaF_2:Mn exposed to UV after the normal read out.

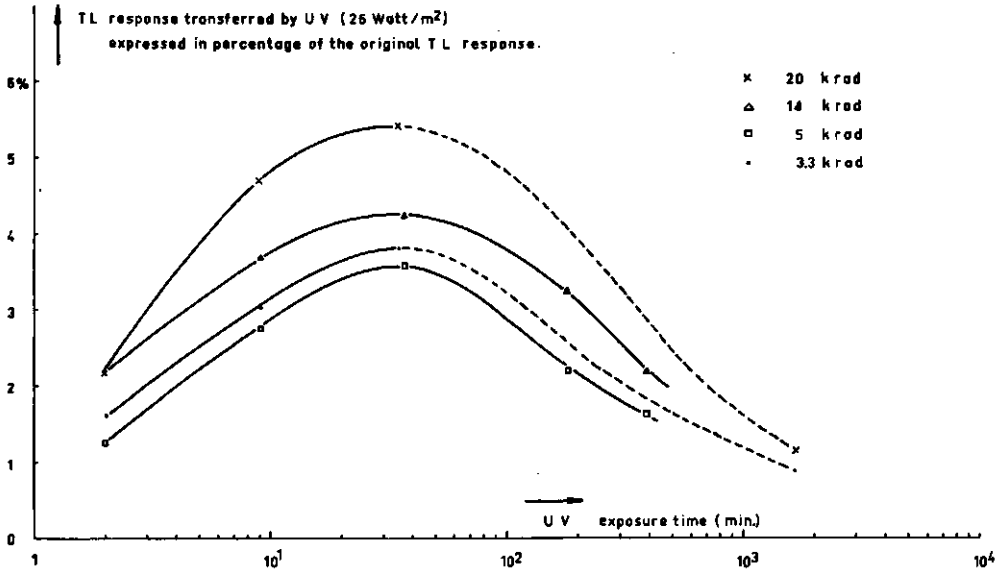

Fig.15. The transferred TL response as a function of various UV exposure times.

The glow curve after a short UV treatment (Figure 14) shows one peak at about 450°C and a second one at about 285°C. The 285°C peak increases with the time of the UV exposure, the 450°C peak remains practically constant.

The transferred TL response as a function of various exposure times (Figure 15) shows a maximum at 30 min. A longer exposure time gives a decrease of the response, whilst a treatment where the powder is exposed to UV for several periods of two minutes, being read out after each exposure, gives a straight line when the results are plotted on a logarithmic time scale (Figure 16).

Likewise a strong fading was observed when irradiated CaF_2:Mn was subjected to UV exposure before the normal read out (Figure 17).

Discussion and Conclusion

The mentioned effects may be explained by assuming a transfer of the trapped electrons from a deeper trap to a trap nearer to the conduction band. The fact that first the traps corresponding to the 450°C peak are filled would indicate this. Also the main peak located at 285°C instead of 260°C shows a direct transfer from one trap into another trap at a somewhat higher energy level. A similar UV effect with natural based

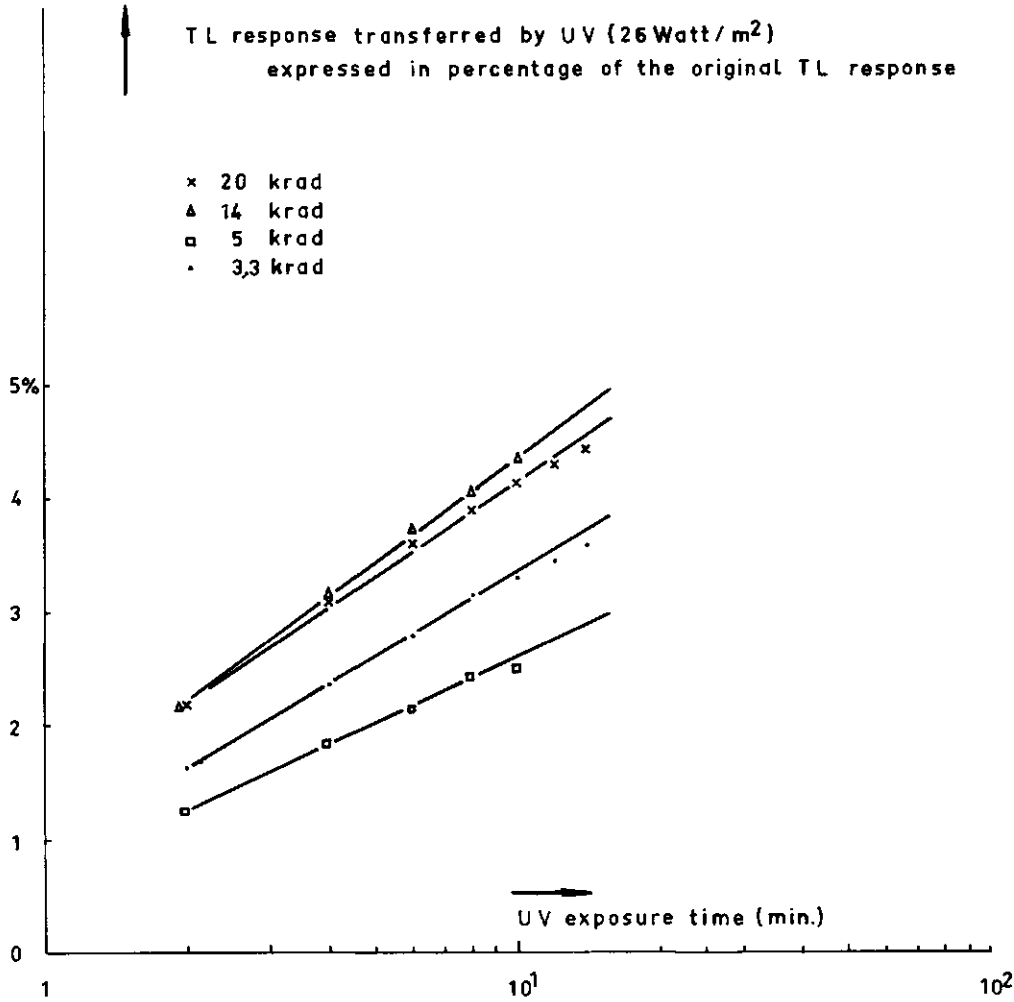

Fig.16. CaF_2:Mn exposed to UV for several periods of two minutes, being read out after each exposure. The sum of the individual responses is plotted against the logarithm of the sum of the UV exposure times.

CaF_2 manufactured at MBLE, Brussels, has already been reported (Brooke and Schayes, 1967).

Because the transferred response is higher for heavy ionizing particles the responsible trapping centers may be created by damage to the crystal during the irradiation. Marrone and Attix (1964) while working with NRL CaF_2:Mn, expect a damage due to gamma irradiation at about 3×10^5 R. The increase in the transferred response for gamma irradiation (Figure 13) starts at about 10^4 rad.

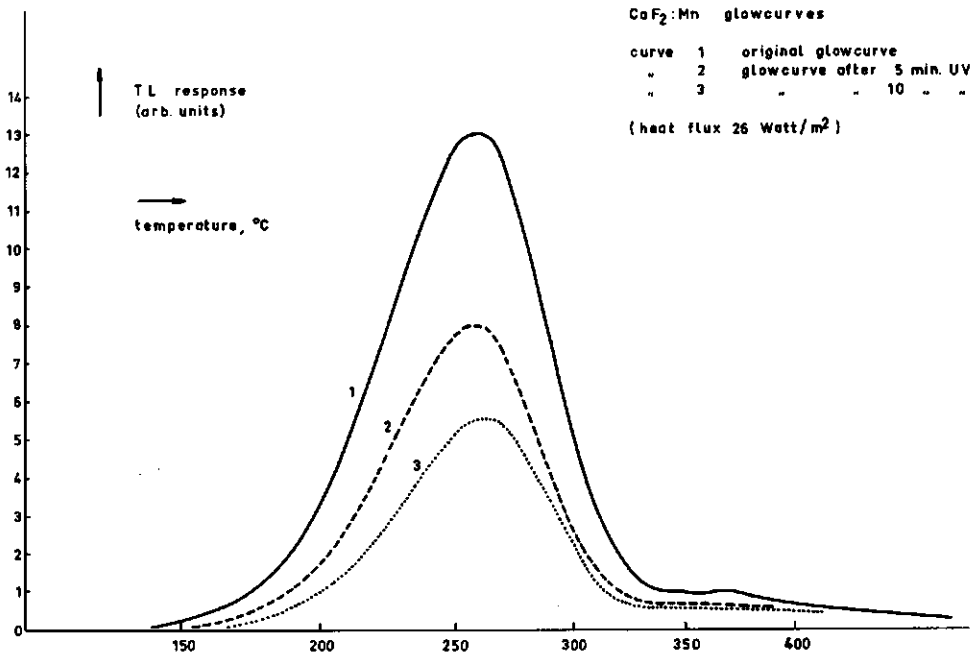

Fig.17. Original glow curve and glow curves of CaF_2:Mn exposed to UV before the normal read out.

ESR measurements [11] have shown that these trapping centers are not located at or near the Mn^{2+} ions.

The height of the main peak at 285°C, close to the original glow peak at 260°C but still separate from it, indicates a great number of trapping centers at the corresponding trap depth. Probably it is one of the single peaks which constitute the composite 260°C peak (Gorbics et al., 1967). A long UV exposure will empty also the traps corresponding to the 285°C peak (Figure 15), resulting in a decrease of the TL response. A transfer between the traps corresponding to the 285°C peak and those corresponding to the 260°C peak has not been observed.

The results of Figure 16 offer the possibility of repeated readings in a very simple way. Another method for repeated readings has been described by Schulman and West (1963). Here the phosphor is heated only part way up the glow curve resulting in a small fraction of the total TL response.

Furthermore, there is a possibility to distinguish between the

11. The ESR measurements have been carried out by Dr. J. Arends (Laboratory for Solid Physics, Groningen).

gamma and heavy particle component of a TL reading because the transferred TL response, expressed in percentage of the original response, is higher in the case of a proton and alpha irradiation. Further investigations are required on this point.

3.3 The sensitivity of CaF_2:Mn for protons and alpha particles

3.3.1 The radiation parameters of the thermal and fast neutron fields

3.3.1A Determination of the thermal neutron flux density by gold foil activation

The irradiation experiments with CaF_2 in a thermal neutron field require a knowledge of the thermal neutron flux density. This information can be obtained through the activation of gold foils (^{197}Au, 100% abundance) at the irradiation position, resulting in radioactive ^{198}Au. The specific saturation activity A_s of these foils can easily be measured with a β-γ coincidence system (Puite and de Swart, 1965).

From the value of A_s the neutron flux density can be calculated knowing the thermal neutron cross section and the number of nuclei per mg. The decay scheme of ^{198}Au is shown in Figure 18 (Aten Jr, 1966). The following data refer to this Figure,

β_1 - E_{max}	= 0.285 MeV,	Intensity/disintegration = 0.012
β_2 -	0.961	0.988
β_3 -	1.373	0.00025
γ_1 - E	= 0.4118	0.955
γ_2 -	0.6759	0.0101
γ_3 -	1.0877	0.0018

The number of electrons emitted/disintegration (β particles + conversion electrons) is 1.043. Of these 0.012 have a low energy with E_{max} = 0.285 MeV.

When the number of β particles which are in coincidence with the 0.412 MeV gamma rays are counted, the following equations can be used:

$$N_\beta(t) = \varepsilon_\beta\, N_o(t)\, 1.043 \qquad N_\gamma(t) = \varepsilon_\gamma\, N_o(t)\, 0.955 \qquad [8;9]$$

$$N_c(t) = \varepsilon_\beta \varepsilon_\gamma\, N_o(t)\, 0.955 \qquad [10]$$

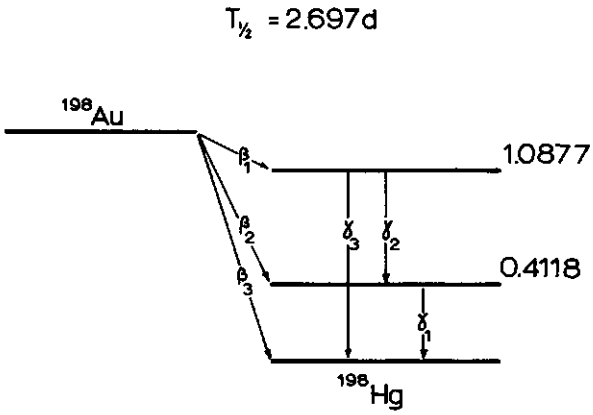

Fig.18. Decay of ^{198}Au.

$N_\beta(t)$, $N_\gamma(t)$ and $N_c(t)$ are the number of counts/sec in the β, γ and coincidence channel, respectively, t sec after the end of the irradiation (decay time t sec). $N_\beta(t)$ has to be corrected for the gamma ray response of the β detector. Accidental coincidence counts should be subtracted to obtain the correct value for $N_c(t)$. ε_β and ε_γ are the total efficiencies of the β- and γ channel, respectively. $N_o(t)$ gives the number of disintegrations/sec (dps) t sec after the end of the irradiation. This value can be calculated from the equations 8, 9 and 10.

The specific saturation activity A_s is then obtained from $N_o(t)$ using the equation

$$A_s = \frac{N_o(t)}{m} \cdot \frac{\exp(\lambda t)}{1 - \exp(-\lambda t_o)} \quad \text{dps/mg} \qquad [11]$$

with m = mass of gold foil in mg.

λ = decay constant of ^{198}Au, being 2.98×10^{-6} sec^{-1}.

t = decay time in sec.

t_o = irradiation time in sec.

The thermal neutron flux density ϕ is,

$$\phi = \frac{A_s}{\sigma N f_{th}} \left(1 - \frac{1}{R_{Cd}}\right) \quad n/s.cm^2 \qquad [12]$$

with σ = thermal neutron cross section for $^{197}Au\ (n,\gamma)\ ^{198}Au$, being 98.8 barn at 2200 m/sec. σ average = $\frac{\pi}{2} \times 98.8$ barn

N = number of ^{197}Au nuclei/mg, being 3.058×10^{18}.

f_{th} = correction factor for thermal self-shielding. For a foil thickness of 90 mg/cm^2 a value of 0.93 has been used.

R_{Cd} = cadmium ratio, defined as the ratio of the saturation activities of a bare and a cadmium covered foil.

The cadmium (σ = 2450 barn) cut-off of an 0.5 mm thick cadmium cover is at approximately 0.5 eV (Hughes, 1953). Epithermal neutrons above this energy cause activation of the gold foils due to the resonance absorption at 4.9 eV. The value of R_{Cd} in the irradiation room of the BARN reactor is $\sim$ 500.

Substitution of the above mentioned values results in

$$\phi = 4.02 \times 10^3 \, A_s \text{ n/s.cm}^2 \qquad [13]$$

with A_s in dps/mg.

The reproducibility of the value for ϕ amounts to $\pm$ 0.4 %. The estimated systematic error is $\pm$ 1.5 %.

To get an impression of the absolute accuracy of the activation measurements, gold foils activated in the BARN reactor with the same neutron fluence were sent to various Institutes in the Netherlands for intercomparison. The results are collected in Table 3. The absolute measurements using β-γ coincidence methods were within $\pm$ 1 %. The results of the measurements where the detectors relied on a calibration were within $\pm$ 5 %.

3.3.1B Determination of the fast neutron spectrum with threshold detectors

The experimental results on CaF_2:Mn irradiated in fast neutron fields can be fruitfully used only, when the fast neutron flux density and the neutron spectrum is known. Threshold detectors, when suitably chosen, may give an indication of this spectrum. Because the cross sections of these foils for the particular spectrum are unknown fission cross sections may be used leading to an equivalent fission flux density.

Four threshold detectors, recommended by IAEA (1967), have been chosen for the comparison of the BARN fast neutron spectrum measured

institute	specific saturation activity A_s(dps/mg)	standard deviation (%)	estimated systematic error (%)	method	measurements carried out by	remarks
RCN Petten	0.9848×10^4 0.9954	±0.25 0.23	2	β γ coincidence	Mr. H.J. Nolthenius	plastic and NaI scintillator
RID Delft	1.0030	0.6		4π β γ coincidence	Mr. J.W. de Vries	proportional flow counter (90% argon and 10% methane), NaI scintillator detector
ITAL, Wageningen	1.006	0.4	1.5	β γ coincidence	Drs. K.J. Puite Mr. J. Huisman Mr. D. Creboldor	plastic and NaI scintillator
Reactor Institute Eindhoven	1.065	0.3		photo peak	Mr. Breimer Mr. van Hout	measuring equipment calibrated with the β-γ coincidence apparatus of RID (Dec. 15th, 1967)
RCN Petten	0.9538 0.9482	0.11 0.19	4	photo peak	Mr. H.J. Nolthenius	data from „Scintillation Spectrometry Gamma-ray Spectrum Catalogue" R.L. Heath (IDO 16880)
Philips Applicatie Laboratorium Eindhoven	0.98	2.5	5	photo peak	Drs. F.E.L. ten Haaf Mr. M.L. Verheijke	NaI scintillation detector, 5 different geometries data from: R.L. Heath (IDO16880), C.E. Crouthamel, Applied gamma ray Spectrometry (1960) M.L. Verheijke, Int. J. appl. Radiat. Isotopes 13, 583 (1962)
RBI - TNO Rijswijk	0.92	1	3		Dr. J.J. Broerse Mr. Engel	^{32}P powder irradiated simultaneously with Au foils Determination of A_s of this powder using a set up calibrated for sulphur pellets. A_s for Au has been calculated using $A_s(Au) = 76.5 \times A_s(P) \pm 3\%$

Table 3. Results of the gold foil activity intercomparison (September 1968).

with these detectors and the spectrometry system (Chadwick and Oosterheert, 1969). Kerma [12] rate values derived from these spectral measurements have been compared with ionization chamber dose rate measurements.

The shape of the spectrum, which is very important for radiobiological experiments (Chadwick et al., 1969), can be altered by partially filling the D_2O diffusor. As the bottom of this tank is hemispherical the influence of different D_2O levels has been measured by using a flat bottomed polypropylene container in the irradiation room above the irradiation position. D_2O levels of 3 and 10 cm were chosen because a fast neutron will make on average one collision in passing through 3 cm of D_2O. The measuring procedure for the different threshold detectors is described briefly:

a. $^{27}Al(n,\alpha)^{24}Na$

The low flux of neutrons having an energy in excess of the threshold energy of 7.0 MeV prohibited the use of β-γ coincidence counting methods. Consequently, only the β emission was measured and the efficiency of the β counter was determined using a β-γ coincidence measurement of an Al foil activated in the reactor core.

b. $^{58}Ni(n,p)^{58}Co$

The activity of the ^{58}Co was determined using a β-γ coincidence method (Dieck, 1966).

c. $^{32}S(n,p)^{32}P$

The counting efficiency for the β particles from ^{32}P has been determined with an accuracy of 4 % using pellets made from sulphur and red phosphor. The red phosphor had previously been activated in a thermal neutron flux.

d. $^{115}In(n,n_1)^{115m}In$

The isomeric transition (0.335 MeV, 95 %) was measured using a NaI crystal in conjunction with a single-channel spectrometer. The efficiency factor was determined using ^{198}Au. An internal conversion factor of 1.045 has been used.

The results of these measurements are presented in the Tables 4 and 5 and Figure 19. The symbols used in Table 4 are defined as follows (Zijp, 1965),

12. The kerma is the energy per unit mass transferred by gamma rays or neutrons into the form of kinetic energy of secondary charged particles at the point of interest in the irradiated material. The kerma factor is the kerma per unit fluence.

Foil	E_{thr} (MeV)	D_2O level (cm)	As (dps/g)	$\langle\sigma_f\rangle$ (mb)	σ_{eff} (mb)	φ_f (n/cm^{2}s)	φ_{eff} (n/cm^{2}s)	$\varphi(E)$ (n/cm^{2}s)	kerma factor T.E. plastic	kerma rate (erg/gs)
^{115}In	1.5	0	7.1×10^4			7.9×10^7	5.4×10^7			
		3	4.6×10^4	179	260	5.1×10^7	3.5×10^7			
		10	3.0×10^4			3.3×10^7	2.3×10^7			
		0						3.8×10^7		12.1
		3						2.6×10^7	3.2×10^{-7}	8.3
		10						1.8×10^7		5.8
^{32}S	2.7	0	7.3×10^4			6.3×10^7	1.5×10^7			
		3	4.4×10^4	65	265	3.8×10^7	9.4×10^6			
		10	2.4×10^4			2.0×10^7	5.0×10^6			
		0						—		—
		3						2.2×10^6	3.7×10^{-7}	0.8
		10						1.7×10^6		0.6
^{58}Ni	2.8	0	5.0×10^4			8.3×10^7	1.6×10^7			
		3	2.5×10^4	100	500	3.6×10^7	7.2×10^6			
		10	1.1×10^4			1.6×10^7	3.3×10^6			
		0						1.5×10^7		6.7
		3						6.6×10^6	4.4×10^{-7}	2.9
		10						3.0×10^6		1.3
^{27}Al	7.0	0	1.1×10^3			8.5×10^7	9.1×10^5	9.1×10^5		0.4
		3	6.8×10^2	0.60	55	5.1×10^7	5.5×10^5	5.5×10^5	4.9×10^{-7}	0.3
		10	4.0×10^2			3.0×10^7	3.3×10^5	3.3×10^5		0.2
total spectrum >1.5		0								19.2
		3								12.3
		10								7.9

Table 4. Calculation of flux density and kerma from threshold detectors for different D_2O filters.

D_2O level (cm)	spectral indices $S_{i/j} = \frac{A_{s,i} / A_{s,j}}{\langle \phi_i \rangle / \langle \phi_j \rangle}$			dose rate (rad/h in tissue)			
				E>1.5		E>0.3	E>0.01
	$S_{In/Al}$	$S_{S/Al}$	$S_{Ni/Al}$	threshold detectors	spectro meter	spectro meter	ionisation chamber
0	0.22	0.61	0.27	690 ±25%	700 ±15%	1100 ±10%	1100 ± 7%
3	0.23	0.60	0.22	440			660
10	0.25	0.55	0.17	280			290

Table 5. Spectral indices and dose rates for different D_2O filters.

A_s = specific saturation activity induced in the detector,

$$A_s = N_o \int^{\infty} \sigma(E)\ \phi_E(E) dE \qquad [14]$$

with N = number of target nuclei per unit of mass

$\sigma(E)$ = differential cross section for the reaction under consideration

$\phi_E(E)$ = fast neutron flux density per unit energy interval.

E_{thr} = threshold energy and

σ_{eff} = effective cross section, defined in such a way that

$$\sigma(E) = 0 \quad \text{for} \quad E < E_{thr}$$

$$\sigma(E) = \sigma_{eff} \quad \text{for} \quad E > E_{thr} \qquad [15]$$

and $$_o\int^{\infty} \sigma(E)\ \phi_E(E) dE = \sigma_{eff} \int_{E_{eff}}^{\infty} \phi_E(E) dE \qquad [16]$$

$\langle \sigma_f \rangle$ = average cross section for a fission spectrum

φ_f = equivalent fission flux density

$$\text{with } \varphi_f = {}_o\int^{\infty} \sigma(E)\ \phi_E(E) dE / \langle \sigma_f \rangle \qquad [17]$$

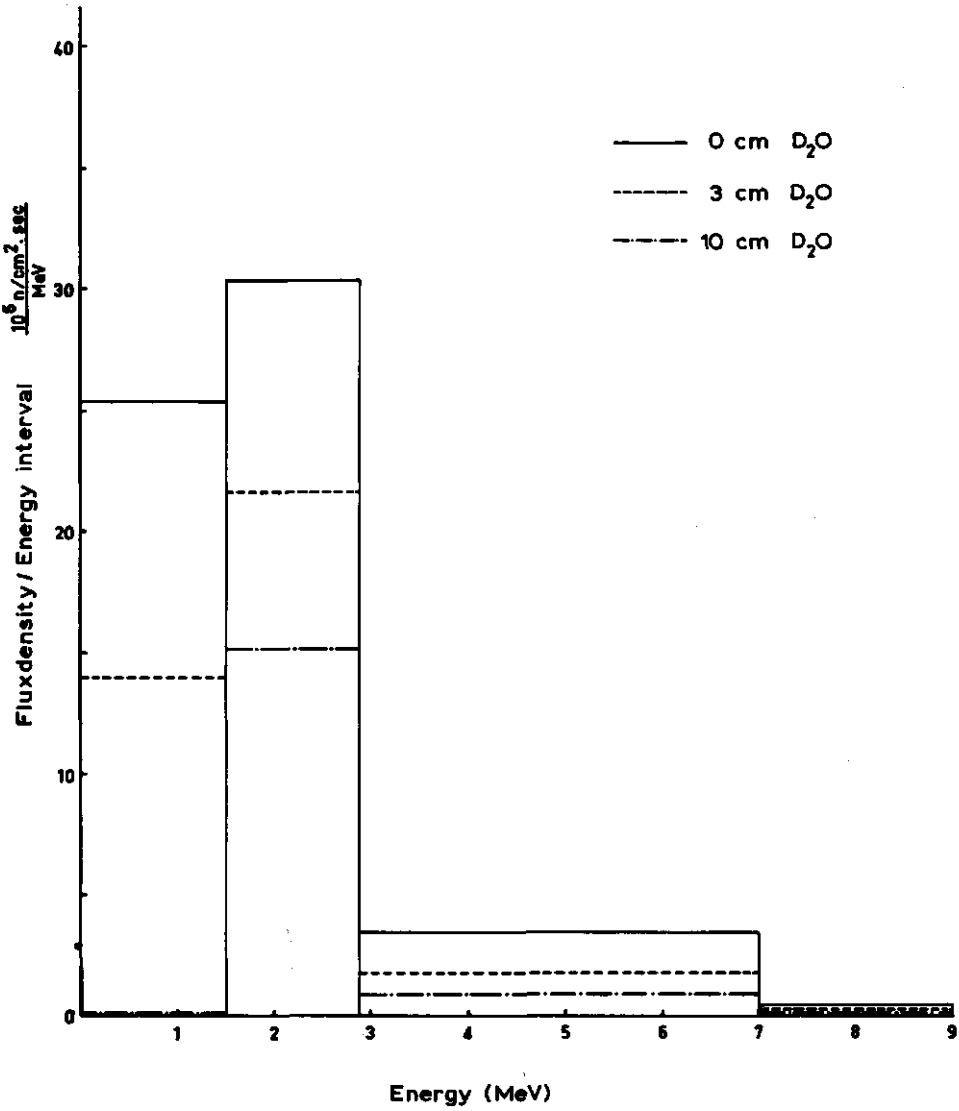

Fig.19. Fast neutron spectrum of the BARN reactor for different D_2O filters.

$\varphi_{eff}(E_{eff},\infty)$ = effective flux density with

$$\varphi_{eff} = \int_0^\infty \sigma(E)\ \phi_E(E)dE\ /\sigma_{eff} \qquad [18]$$

This is a measure of the flux density above the threshold energy.

$\varphi(E) = \Delta.\varphi_{eff}$ in ΔE

The change in spectral shape caused by the D_2O filters is indicated in Figure 19. At energies above 1 MeV the results have been directly calculated from the flux densities given in Table 4 and an estimate of the flux densities below 1.5 MeV has been obtained using a kerma factor of 3×10^{-7} erg/g per unit fluence by comparing the kerma rates calculated from the flux densities above 1.5 MeV and the dose rates measured by the ionization chambers. The justification for this procedure comes from Table 5 where it can be seen that there exists a good correlation between the spectrometer and threshold detectors above 1.5 MeV and between the spectrometer and ionization chambers over the total energy spectrum.

As the scattering cross section of deuterium increases for lower energy neutrons it may be expected that these neutrons will be more efficiently thermalised resulting, as shown in Figure 19, in a spectrum which becomes sharper and where the peak moves up to higher energy.

3.3.2 Thermoluminescent response of CaF_2:Mn mixed with organic liquids in thermal and fast neutron fields

published before in Health Physics, 1969, vol. 17, pp. 661-667.

Introduction

The difference in the thermoluminescence of dry powder and powder mixed with a liquid irradiated in a neutron field is due to the contribution of charged particles, which are created by the neutron interaction with the liquid and which deposit part of their energy in the powder.

Previously attempts have been made by others to increase the ^{7}LiF reading in a fast neutron field by mixing the ^{7}LiF with alcohol or other hydrogenous liquids (Karzmark et al., 1964; Wingate et al., 1965) and to use these systems for fast neutron dosimetry (Unruh et al., 1967). Because the gamma ray response of the wet dosimeter was different from that of the dry dosimeter and because it was not possible to equalize this response by the use of a non-hydrogenous liquid a practical dosimetry system with LiF has not yet been developed (Unruh et al., 1967).

The aim of the work described here was to investigate the thermoluminescent (TL) response of CaF_2:Mn, irradiated in a neutron field of a reactor, when the powder was mixed with different liquids during irradiation.

CaF_2 was mixed with different mixtures of acetone-acetonitrile and alcohol-boric acid to investigate the TL response caused by the $^{14}N(n,p)^{14}C$ and the $^{10}B(n,\alpha)^{7}Li$ reactions occurring during a thermal neutron irradiation. In a fast neutron irradiation the CaF_2 was mixed with alcohol to determine the TL response due mainly to the proton recoil reaction.

CaF_2 powder was chosen because it may be expected to have a low neutron sensitivity and in fact it showed in these experiments no detectable neutron sensitivity. Handloser (1965) has reported a sensitivity for thermal neutrons of 1.4×10^{-10} R per n/cm^2 and 1.1×10^{-10} R per n/cm^2 for 5.4 MeV neutrons. Tochilin et al. (1969) obtained a value of 0.58 $\times 10^{-10}$ R per n/cm^2 for thermal neutrons. However, the results presented here are unaffected by a possible neutron sensitivity of the CaF_2.

Materials and Methods

The CaF_2:Mn powder has been manufactured at the Philips laboratories, the Netherlands (Puite, 1968). The crystal diameter is 10-15 μm. Small teflon tubes, each containing 100 mg CaF_2 and 0.55 cm^3 of liquid were irradiated in the climate controlled room under the core of the BARN reactor (Bogaardt et al., 1964) or in the open 300 Ci ^{137}Cs gamma field at ITAL. The tubes were filled 100-120 h before irradiation, because preliminary experiments demonstrated that the pre-irradiation filling time is important for the reproducibility of the results. During this pre-irradiation filling time and also during irradiation the tubes were rotated to maintain a good contact between the powder and the liquid.

Immediately after irradiation the liquid was removed and the wet powder was allowed to dry at room temperature in the dark. All TL readings were made two days after the end of the irradiation to be sure that the powder was completely dry and to avoid a variation of the readings due to the fading of the TL signal. This fading is negligibly small two days after irradiation (Schulman, 1967). The planchet, containing 45 mg of the powder, was heated to 400°C in a modified Con-Rad Model 4100 TLD read-out instrument at a rate of 2.7°C/sec, and the integrated light signal was measured.

The thermal neutron flux density has been determined by the activation of a gold foil placed inside one of the teflon tubes. The inherent gamma contamination of the thermal neutron flux has been

measured with a teflon-CO_2 ionization chamber. The fast neutron dose and the gamma contamination of the fast neutron flux have been determined using acetylene equivalent and magnesium-argon ionization chambers. In order to obtain the fast neutron dose in alcohol, the fast neutron dose measured with the acetylene equivalent chamber has been multiplied with the factor 1.59 (IAEA, 1967).

Experimental Results

CaF_2:Mn and liquids in a thermal neutron field

Teflon tubes with CaF_2 powder mixed with mixtures of acetone (C_3H_6O)-acetonitrile (C_2H_3N) and of alcohol (C_2H_6O)-boric acid (H_3BO_3) have been irradiated in a thermal neutron field. The amount of nitrogen and boron in the mixtures was varied between 0 and 34 % of nitrogen and 0 and 400 ppm of boron by weight. The fluence varied between (1.6-7.6) x 10^{12} n/cm^2 and the accompanying gamma contamination of the neutron irradiation amounted to 200-760 rad in tissue depending upon the irradiation position and the irradiation time (24-54 h). The absorbed doses in the liquids due to the reactions $^{14}N(n,p)^{14}C$ and $^{10}B(n,\alpha)^{7}Li$ have been calculated using 7.6 x 10^{-12} rad per weight percentage of nitrogen per n/cm^2 and 157 x 10^{-12} rad per weight percentage of boron per n/cm^2 (IAEA, 1967). The TL readings corrected for gamma and neutron dose have been plotted against the proton plus carbon recoil and alpha plus lithium recoil doses in the liquids (Figures 20 and 21). From these results one may derive a TL reading of 20.5 $\pm$ 1.2 mV/krad proton plus carbon recoil dose and 14.8 $\pm$ 0.7 mV/krad alpha plus lithium recoil dose in the liquids. These values may be compared with a reading of 450 mV/krad for dry CaF_2 irradiated in a ^{137}Cs gamma field based on the absorbed dose in muscle tissue.

Dry CaF_2 has been included in this series and rotated in the same way. The TL readings of this dry CaF_2 and of CaF_2 mixed with acetone and alcohol have been compared with the readings obtained from similar irradiations in a ^{137}Cs gamma field using the same doses and dose rates as the gamma contamination during the thermal neutron irradiations. In all three cases a lower reading was found when the irradiations took place in the thermal neutron field. The data are collected in Table 6.

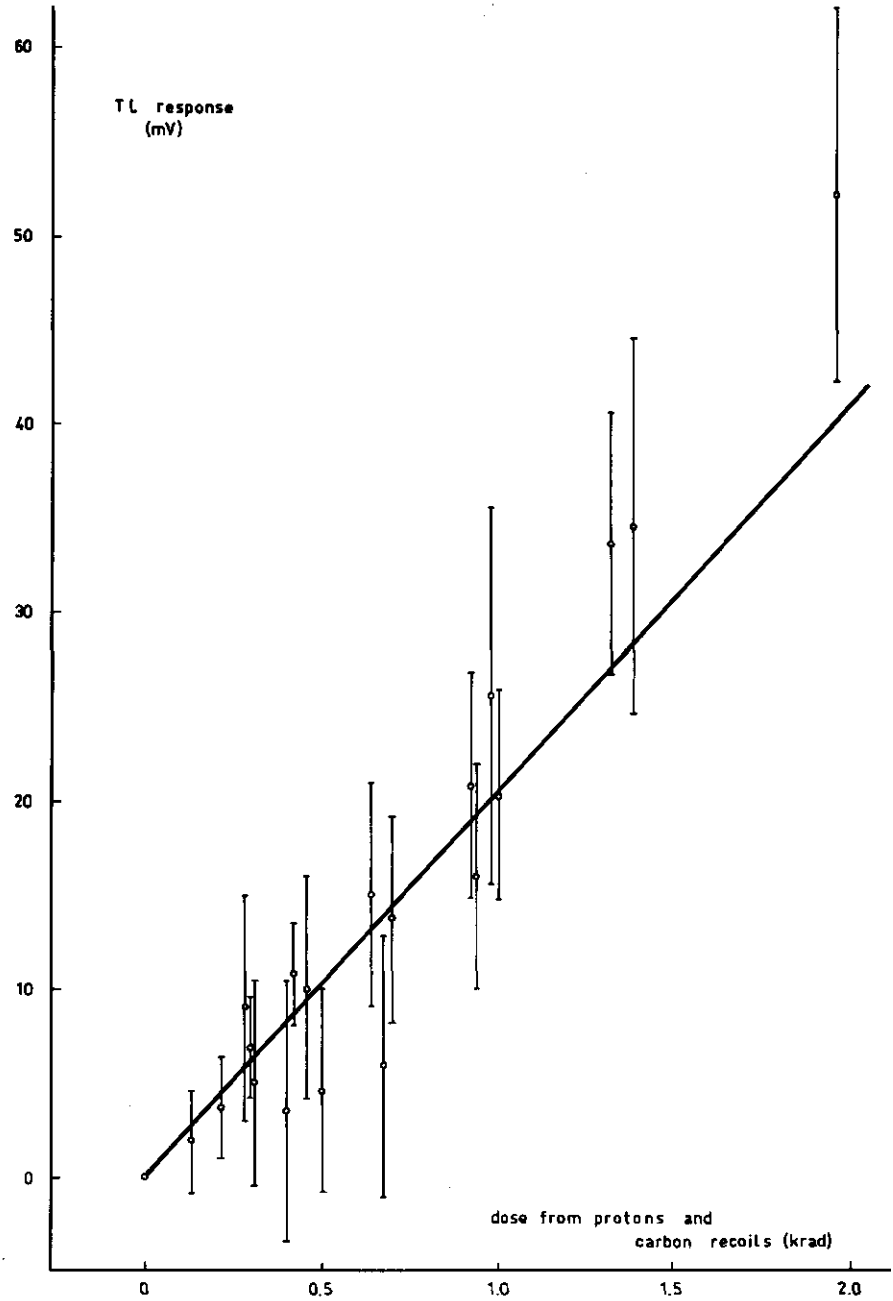

Fig.20. The TL response of CaF_2:Mn mixed with mixtures of acetone-acetonitrile during a thermal neutron irradiation and due to the protons and carbon recoils from the ^{14}N (n, p)^{14}C reaction, occurring in the liquid, as a function of the dose delivered by these charged particles in the liquid.

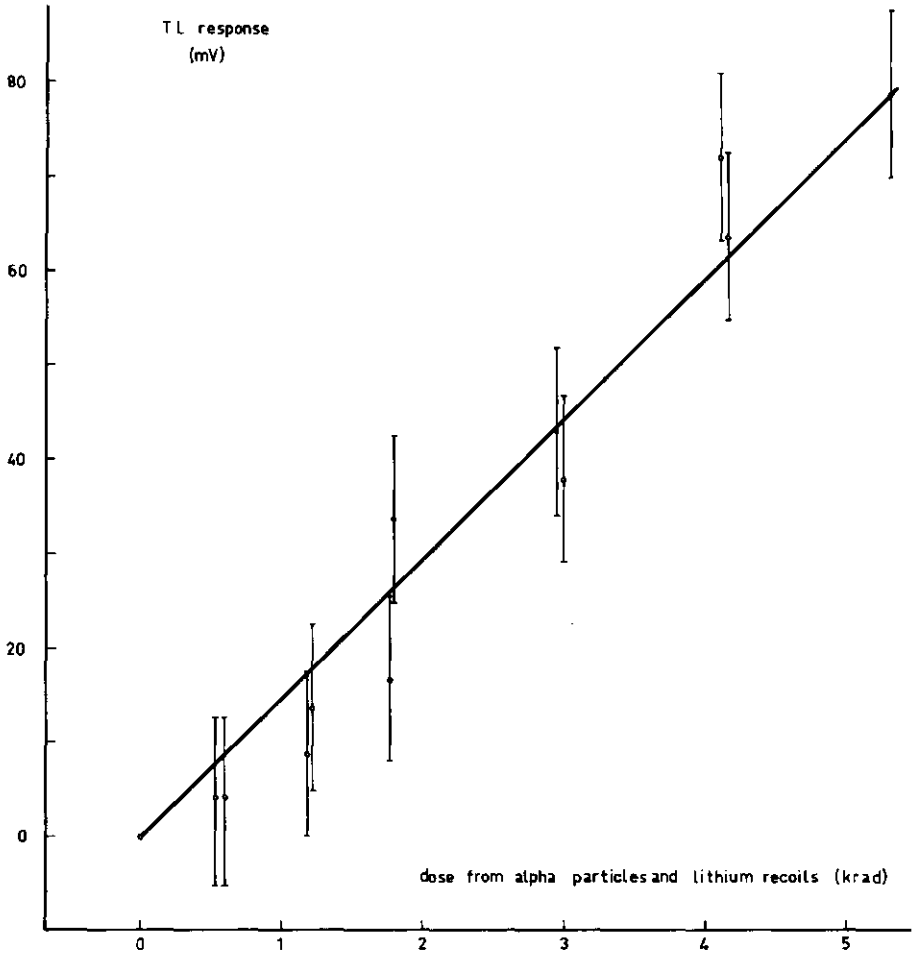

Fig.21. The TL response of CaF_2:Mn mixed with mixtures of alcohol-boric acid during a thermal neutron irradiation and due to the alpha particles and lithium recoils from the ^{10}B (n, α)^{7}Li reaction, occurring in the liquid, as a function of the dose delivered by these charged particles in the liquid.

Material	Ratio in %
dry CaF_2	66 ± 4
CaF_2 mixed with acetone	78 ± 5
CaF_2 mixed with alcohol	69 ± 4

Table 6. The ratio of the TL response due to gamma rays and thermal neutrons of CaF_2 irradiated in a thermal neutron field compared with similar irradiations in a gamma field.

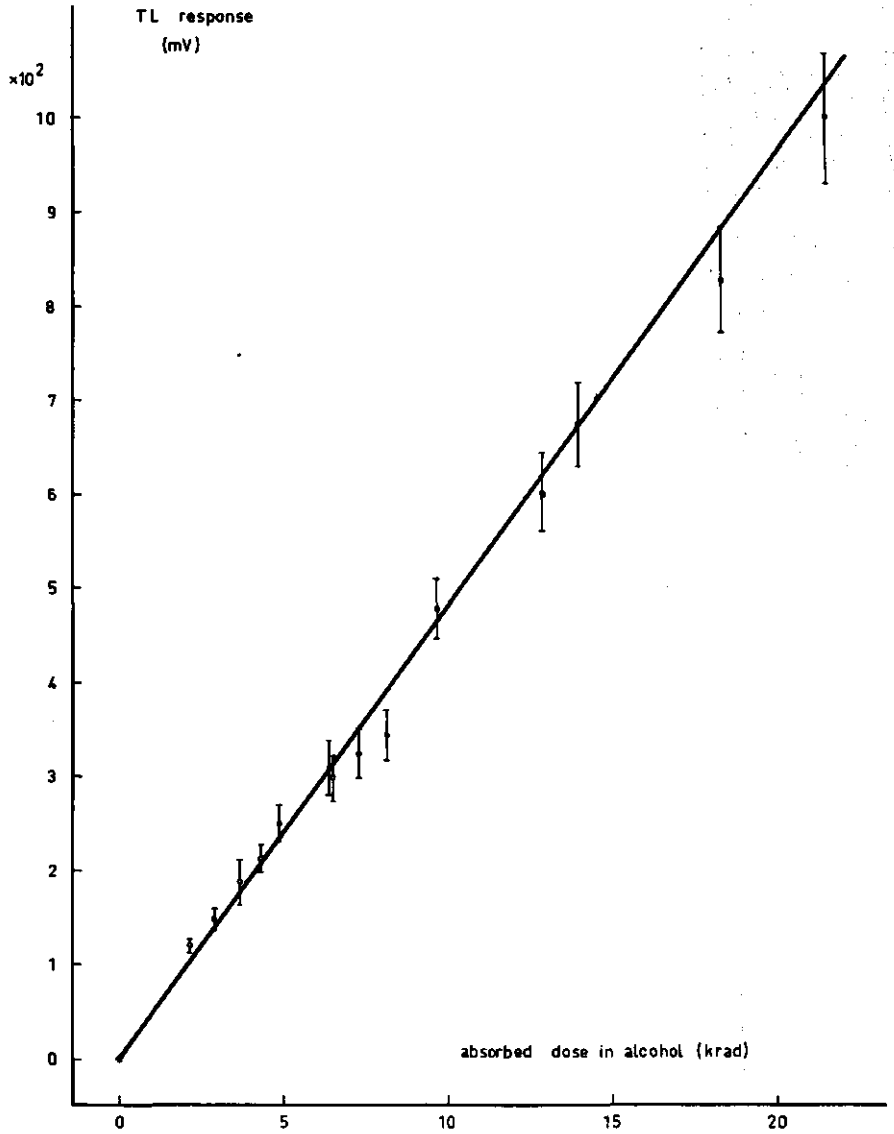

Fig.22. The TL response of CaF_2:Mn mixed with alcohol during a fast neutron irradiation and mainly due (92.5 %) to the proton recoil reaction, occurring in the alcohol, as a function of the fast neutron dose in the alcohol.

Material	Ratio in %
dry CaF_2 rotated	65 ± 2
dry CaF_2 not rotated	66 ± 3

Table 7. The ratio of the TL response due to gamma rays and fast neutrons of CaF_2 irradiated in a fast neutron field compared with similar irradiations in a gamma field.

CaF_2:Mn and alcohol in a fast neutron field

Teflon tubes with CaF_2 mixed with alcohol have been irradiated in a fast neutron flux at different reactor powers for 5.5 h. Tubes filled with dry powder have been included in these series. Two different irradiation positions have been used where at maximum reactor power the fast neutron dose rates in acetylene were 2440 rad/h and 925 rad/h and the gamma contamination was 170 rad/h and 87 rad/h, respectively.

In order to separate the TL reading due to the contribution of the recoils produced in the alcohol from the total TL reading the following procedure has been followed: similar irradiations with dry CaF_2 and CaF_2 mixed with alcohol have been carried out in a ^{137}Cs gamma field using the same doses and dose rates as the gamma contamination during the fast neutron irradiation. In this way the ratio of the readings of the wet to the dry powder has been determined (0.93 ± 0.03). The reading of the dry CaF_2 irradiated in the reactor field has been multiplied with this factor and subtracted from the readings of the CaF_2 mixed with alcohol which has been irradiated in the reactor field. The difference in the readings has been attributed to the response of the recoils produced in the alcohol; proton recoils contribute 92.5 % of the absorbed dose in the alcohol. The results have been plotted in Figure 22 and show a TL reading of 47.6 ± 0.9 mV/krad absorbed dose of the recoils in the alcohol.

This procedure assumes that the reduction in sensitivity caused by the fast neutrons (see Table 7) is the same in dry CaF_2 and in CaF_2 mixed with alcohol. There is no evidence for or against this assumption. The value of 47.6 mV/krad may also be compared with the reading of 450 mV/krad for dry CaF_2 irradiated in a ^{137}Cs gamma field based on the absorbed dose in muscle tissue.

The readings of dry CaF_2 irradiated in the fast neutron field have been compared with those of dry CaF_2 irradiated in the ^{137}Cs gamma field using the same doses and dose rates as the gamma contamination during the fast neutron irradiation. Lower readings were obtained when the irradiations took place in the fast neutron field. The data are collected in Table 7.

Discussion and Conclusion

Consistent results were only obtained in these experiments when a

considerable pre-irradiation filling time was used. One explanation for this could be that in the final stage of preparation the CaF_2 is milled and sieved and this introduces a large number of defects in the surface of the crystals, resulting in the formation of an amorphous layer. This layer is easily attacked by the surrounding liquid and etch pits will be created. Patel and Desai (1965,1968) reported that the rate of increase in the size of the etch pits does not remain constant but decreases as the powder is progressively etched, consequently, the influence of the liquid on the crystal surface decreases with etching time. If the TL response is dependent on crystal surface changes, a filling time before irradiation will thus reduce the influence of the liquid on the crystal surface during irradiation and also the dependence of the TL response on the irradiation time. The importance of the effect of crystal surface changes on the TL signal has been demonstrated by Carter et al. (1963) and Zanelli (1968). Carter et al. found a remarkable dependence of the TL response of KCl and NaCl with sample surface area and Zanelli has reported an effect of particle size on the thermoluminescence of LiF.

The thermoluminescent response of CaF_2 per krad for the alpha particles plus lithium recoils, the protons plus carbon recoils and the proton recoils, produced in the surrounding liquids during neutron irradiation, compared with the response of dry unrotated CaF_2 per krad irradiated in a pure gamma field was found to be 3, 5 and 11 %, respectively. These results obviously can not be compared with the TL efficiency of 9 % reported from ^{210}Po alpha particle bombardment experiments (Woodley and Johnson, 1967), because the experimental procedures are not the same.

The TL readings of dry CaF_2 irradiated in a thermal or fast neutron field are 65 % of the readings obtained from a ^{137}Cs gamma irradiation using the same doses and dose rates as the gamma contamination during the neutron irradiations. This effect cannot be explained by the energy dependence of CaF_2.

Oltman et al. (1967) have reported a lower gamma sensitivity for ^{7}LiF in a mixed neutron-gamma field and suggest that neutrons of less than 1 MeV could introduce lattice vibrations similar to the thermal effect during the heating up of the powder.

A possibility exists that the TL response produced by the charged particles is also reduced by neutron interference. In this case the TL response for a fixed charged particle dose should decrease as the

neutron fluence is increased. It is possible to conclude that such a dependence does not exist in the present experiments with thermal neutron irradiations. It is remarkable that the thermal neutron as well as the fast neutron irradiation both give the same percentage reduction in TL response. The ratio of the flux density ($n/s.cm^2$) to the gamma contamination (rad/sec) has been calculated and amounts for the thermal neutron irradiation 8×10^9 n/cm^2.rad and for the fast neutron irradiation 6×10^9 n/cm^2.rad. Measurements will be carried out to investigate if this ratio determines the extent of the percentage drop in TL response.

It may be concluded from the results obtained till now that CaF_2 cannot be used to measure the gamma contamination of a neutron field. This fact restricts the use of CaF_2 mixed with liquids as a dosimetry system in neutron irradiations.

3.4 The sensitivity of CaF_2:Mn for thermal and fast neutrons

accepted for publication by 'Health Physics' as 'Thermoluminescent sensitivity of CaF_2:Mn in a mixed neutron-gamma field'.

Introduction

Thermoluminescent (TL) powders are often used in mixed neutron-gamma fields in order to determine the neutron sensitivity of the phosphor or to evaluate the gamma component of the irradiation field (Handloser, 1965; Mason, 1970; Endres and Kocher, 1968; Reddy et al., 1969). Experiments (Puite, 1969) with CaF_2:Mn have given TL yields in a mixed neutron-gamma field which were lower than expected.

Results reported for ^{7}LiF (Oltman et al., 1967) with neutron fluences up to 4×10^8 n/cm^2 showed, that when ^{7}LiF was pre-exposed to gamma rays followed by a fast neutron irradiation or exposed simultaneously to fast neutrons and gamma rays a TL yield was obtained, which was lower than the sum of the responses from the neutron and gamma components separately. Further experiments with 6-14 MeV neutrons (Kastner et al., 1969) for fluences of approximately 10^8 n/cm^2 indicated that the decrease in TL signal was mainly due to permanent damage and not to lattice heating. In other LiF dosimetry powders and in $Li_2B_4O_7$:Mn a significant reduction of response was also observed when these powders were irradiated by gamma rays followed by a fast neutron fluence of 3.8×10^9 n/cm^2 (Wallace and

Ziemer, 1968).

The aim of the work described here was to study the TL sensitivity of CaF_2:Mn in a mixed field of neutrons and gamma rays as a function of both components of the irradiation. A possible explanation for the observed drop in TL sensitivity is given for the case of a mixed fast neutron - gamma field, which leads to a mathematical expression for the TL sensitivity in mixed fast neutron - gamma fields.

Methods

CaF_2 powder doped with 4.1 mole % of manganese (Philips, the Netherlands) has been irradiated at different heights in the climate controlled room under the core of the BARN reactor at Wageningen (Chadwick and Oosterheert, 1969). In this reactor a D_2O diffusor is situated between the core and the irradiation room. Thermal neutron irradiations are made with the D_2O diffusor full and fast neutron irradiations are made with the diffusor empty. To remove any thermal neutron contamination of the fast neutron beam a boron shield is inserted between the two bismuth gamma shields, which are situated under the diffusor. Thermal neutron as well as fast neutron irradiations have been carried out with irradiation times from 3-65 h.

The thermal neutron fluence, measured by gold foil activation, varied from 2.5×10^{11} to 1.0×10^{13} n/cm^2 with an accompanying gamma contamination of 34 to 530 rad in tissue, determined with a magnesium-CO_2 ionization chamber.

The fast neutron dose and the inherent gamma contamination have been determined using acetylene equivalent and magnesium-argon ionization chambers. The neutron dose (for CH) varied between 1.5 and 208 krad, being equivalent -using the BARN spectrum data- to 7×10^{11} and 9×10^{13} n/cm^2 and the gamma dose varied between 0.2 and 12 krad in tissue. The fast neutron doses quoted in this paper are related to acetylene and the gamma doses refer to soft tissue material.

The CaF_2 powder was not annealed prior to use because no back-ground signal was observed from an unirradiated sample. During and after the irradiations the powder was kept in the dark. All TL readings were carried out two days after irradiation to avoid a variation in the readings due to fading of the signal. The powder was heated to 370°C at a rate of 2.7°C/sec in a modified Con-Rad Model 4100 TLD reader and the

integral signal was measured.

Experimental Results

Thermal neutrons

The results of the thermal neutron experiments are shown in Figure 23. Only (n,γ) reactions are involved and consequently the

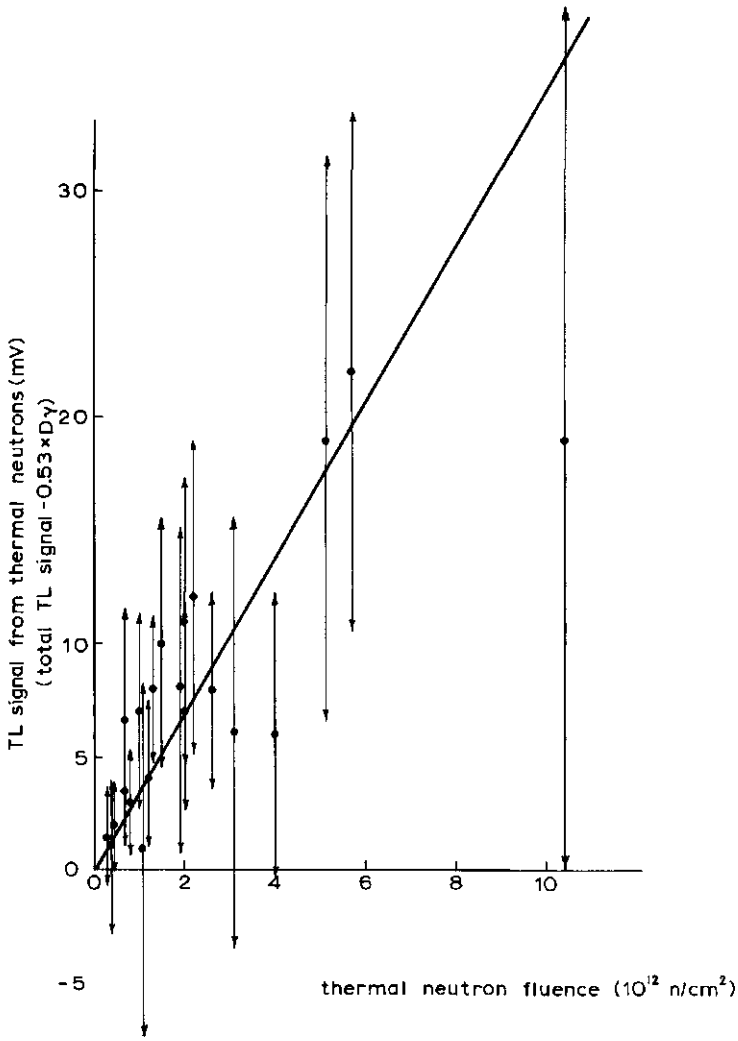

Fig.23. TL signal of CaF_2:Mn from thermal neutrons as a function of the thermal neutron fluence.

linear expression

$$TL = a\ D_\gamma + b\ \emptyset t \qquad [19]$$

has been assumed

with D_γ = gamma dose in rad (rad_γ)

$\emptyset t$ = thermal neutron fluence in n/cm^2

and a = 0.53 ± 0.01 mV/rad (from gamma calibration curve).

A linear regression calculation[13] yielded b = 0.035 ± 0.004 mV per 10^{10} n/cm^2, resulting in a thermal neutron sensitivity of 0.07 ± 0.01 rad_γ per 10^{10} n/cm^2. The errors shown in Figure 23 are large because the thermal neutron signal arises from the subtraction of two large values.

Powder irradiated in thermal neutron fluences up to 4×10^{12} n/cm^2 and following read out irradiated with ^{137}Cs gamma rays did not show a change in the gamma ray TL sensitivity. No special annealing procedure was used between the thermal neutron irradiation and the exposure to ^{137}Cs gamma rays apart from the normal read out up to 370°C.

Fast neutrons

The results of the fast neutron experiments show that as the fast neutron dose increases the TL response associated with the fast neutrons decreases (Figure 24). They fit the expression

$$TL = a\ D_\gamma + b\ D_n \qquad [20]$$

with D_n = fast neutron dose in rad in CH (rad_n).

A linear regression calculation with a = 0.53 ± 0.01 mV per rad_γ yielded:

b = $-\ (0.0102 \pm 0.0004)$ mV per rad_n in CH

resulting in b/a of -0.019 rad_γ/rad_n in CH, equivalent to -0.43 rad_γ per 10^{10} n/cm^2.

13. Part of the computations have been carried out at the Statistical Department ABW-TNO, Wageningen, for which thanks are especially expressed to Ir. A. Heyting of this Department.

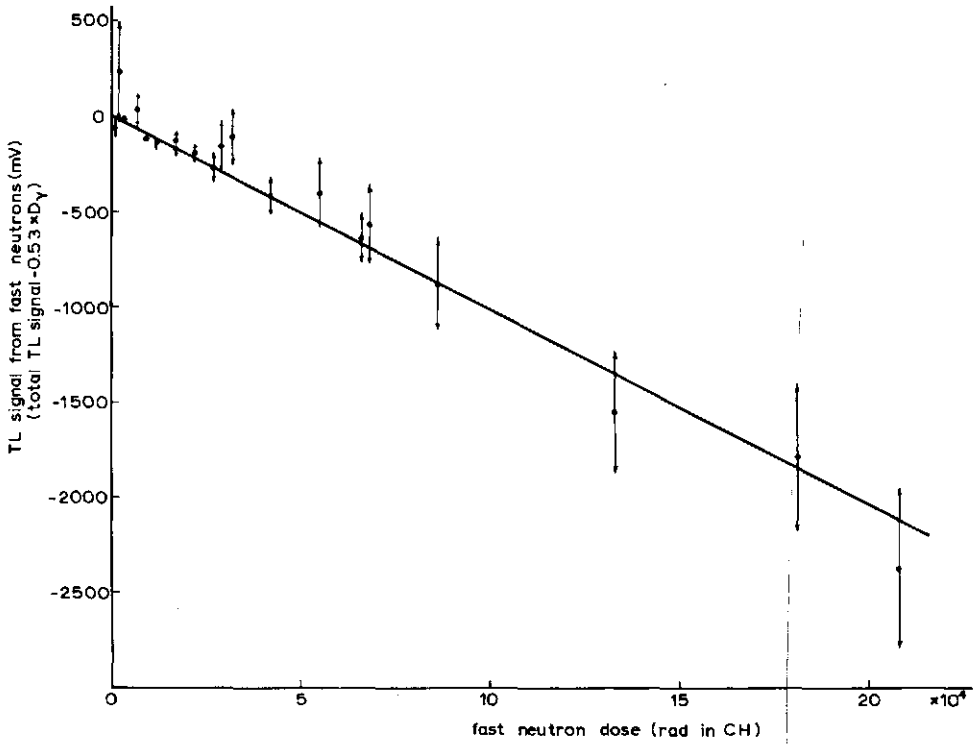

Fig.24. TL signal of CaF_2:Mn from fast neutrons (average neutron energy 1.7 MeV) as a function of the fast neutron dose.

Dose rate experiments (25 h at 10 kW, 10 h at 25 kW, 5 h at 50 kW and 2.5 h at 100 kW) confirmed that the results were independent of the neutron dose rate.

When CaF_2 powder was irradiated with fast neutrons up to D_n = 180 krad, read out and irradiated afterwards with ^{137}Cs gamma rays no change in the gamma ray TL sensitivity was observed.

In Table 8 the relative TL readings are shown of CaF_2 irradiated with ^{137}Cs gamma rays followed or preceded by a fast neutron irradiation. The procedure was as follows. The CaF_2 powder was divided into four parts (A, B, C and D). Parts A and B were subjected to a gamma dose D_γ. After irradiation, part B was read out and then all four parts were exposed to a neutron dose D_n. After reading out part D, parts C and D were irradiated with a gamma dose D_γ, which was the same as initially given to parts A and B.

The above procedure has been carried out in four series I to IV with neutron- and gamma doses varying between 3 to 80 krad and 0.3 to 3.7 krad,

irradiation procedure	relative TL reading			
	series I	II	III	IV
A. gamma irradiation followed by a fast neutron irradiation	96	98	101	97
B. As A, but a TL readout in between the two irradiations	54+46 (100)	54+45 (99)	52+47 (99)	54+45 (99)
C. fast neutron irradiation followed by a gamma irradiation	102	98	101	99
D. As C, but a TL readout in between the two irradiations	46+54 (100)	45+55 (100)	47+53 (100)	45+55 (100)

Table 8. Relative TL reading of CaF_2:Mn irradiated with gamma rays followed or preceded by a fast neutron exposure.

respectively. The readings were normalized for the case of D in Table 8.

The differences in TL responses as shown in Table 8 were not significant.

Discussion

Thermal neutrons

The TL response of CaF_2 irradiated in a mixed thermal neutron-gamma field can be considered to be the sum of the TL responses of the two components of the irradiation field over the dose and dose rate range mentioned.

In earlier experiments (Puite, 1969) with CaF_2, rotated during irradiation, a lower TL response was found when the powder was irradiated in a thermal neutron field compared with a pure gamma irradiation using the same dose as the dose of the gamma contamination of the neutron field. More recent experiments have indicated the possibility that the measurements made with the ionization chamber close to the rotating teflon cylinder overestimated the gamma dose which the powder in the teflon containers inside the cylinder actually received. This may explain the difference between the gamma ray response in a mixed thermal neutron - gamma field presented here and that presented in a previous publication (Puite, 1969).

The thermal neutron sensitivity of CaF_2:Mn barely exceeds the experimental error and is small compared to sensitivities reported for other powders, including ^7LiF (Reddy et al., 1969).

Fast neutrons

Fast neutrons will mainly produce heavy ion recoils (Ca and F ions) through elastic collisions in the CaF_2. These recoils loose their energy in excitation and ionization of the lattice ions, in displacement production and lattice vibrations.

A threshold energy E_i can be defined (Billington and Crawford, 1961) in such a way that when the Ca and F recoils have a primary energy $E_p > E_i$ they loose most of their energy by ionization and excitation. When $E_p < E_i$ nearly all the energy is lost by elastic collisions, resulting in displacements and lattice vibrations. For the Ca and F ions E_i is $\sim$ 90 and 40 keV, respectively. The neutron energy corresponding to this threshold energy E_i can be calculated to be 3 and 0.7 MeV for Ca and F ions, respectively.

It can be estimated (Billington and Crawford, 1961) that in CaF_2 300 to 400 ions will take part in one displacement cascade. Due to recombination only a small fraction of these defects will be permanent and will compete with the dosimetry traps for the electrons. These defect traps will not necessarily have the same properties as the traps emptied during normal TL read out.

Model of thermoluminescent sensitivity for fast neutrons

In order to explain the results obtained the following model is proposed:

Let T_D = number of electrons captured by dosimetry traps in CaF_2:Mn at a dose D, where $D = AD_\gamma + BD_n$.

N_o = maximum number of dosimetry traps.

α = probability of filling a dosimetry trap per unit dose.

T_p = number of neutron induced permanent electron traps P created during the displacements. $T_p = g\ D_n$, with g = constant.

As a result of the evidence presented in Table 8 it may be assumed that all the P traps are filled i.e. no influence of the neutron formed P traps is observed when neutron irradiated CaF_2 is exposed to gamma rays. This implies that the P traps have a very large trapping cross section for electrons compared with the dosimetry traps. The properties of the P traps are also assumed to be such that they will not be emptied during the TL read out procedure.

Because the number of electrons trapped in P traps will reduce the number available for the dosimetry traps, it follows that

$$dT_d = \alpha\ (AdD_\gamma + BdD_n - gdD_n)\ (N_o - T_D) \qquad [21]$$

Integration of equation 21 leads to

$$T_D = N_o\ (1 - \exp\ (-\ \alpha\ [AD_\gamma + BD_n - gD_n])) \qquad [22]$$

For $\alpha\ [AD_\gamma + BD_n - gD_n] << 1$ equation 22 can be written as

$$T_D = \alpha N_o\ (AD_\gamma + BD_n - gD_n) \qquad [23]$$

The TL signal, being proportional to T_D, can be written as

$$TL = aD_\gamma + b'D_n - cD_n \ = \ aD_\gamma + bD_n \qquad [24]$$

with $a/b'/c = A/B/g$ and with $b = b' - c$

According to the literature b/a would be defined as the fast neutron sensitivity although following the arguments presented here b contains a positive sensitivity b' and a negative effect c due to the formation of P traps. The value of b has been found to be negative and this means that for the fast neutron spectrum used in this work the formation of P traps plays an important role.

The filled permanent traps P do not influence the TL sensitivity of CaF_2 for subsequent gamma irradiations as can be seen from Table 8. Similar results for CaF_2 as mentioned in this table have been obtained by Bewley (1969). ^7LiF, however, exhibits a lower TL sensitivity for gamma rays after a fast neutron exposure (Kastner et al., 1969). This is probably due to interference between the TL process and the neutron induced permanent damage traps, already present.

It is also reasonable to assume that the filled dosimetry traps in the CaF_2 present in a disordered region will release their electrons due to lattice vibrations. This effect will not be important for fast neutron fluences up to 10^{14} n/cm^2, but may have a marked influence on the TL signal if fluences of 10^{17} n/cm^2 or higher are used.

Comparison of neutron sensitivities

Some recently reported neutron sensitivities for CaF_2 are collected in Table 9.

The thermal neutron sensitivity of CaF_2:Mn is in part determined by the manganese which has a relatively important macroscopic cross section. Thus, in order to compare the thermal neutron sensitivities of the different CaF_2:Mn samples given in Table 9 the manganese concentration must be known.

type of irradiation	sensitivity in rad per 10^{10} n/cm^2	reference	origin or manufactory
thermal	0.58	Tochilin et al.,1969	EG and G, hot pressed
	approx. 0.2	Ayyangar et al,1968	Con.Rad, disks
	approx. 0.10 - 0.13	Reddy et al,1969	Harshaw, powder
	0.07	this paper	Philips, powder (4.1 mole % Mn)
1.7 MeV (average energy BARN spectrum)	-0.43	this paper	Philips, powder
5.4 MeV	1.1	Handloser, 1965	EG and G, powder
14.0 MeV	14.7	Handloser, 1965	EG and G, powder
14.7 MeV	15	Goldstein et al., 1970	EG and G, hot pressed

Table 9. Neutron sensitivities of CaF_2:Mn expressed in rad per 10^{10} n/cm^2.

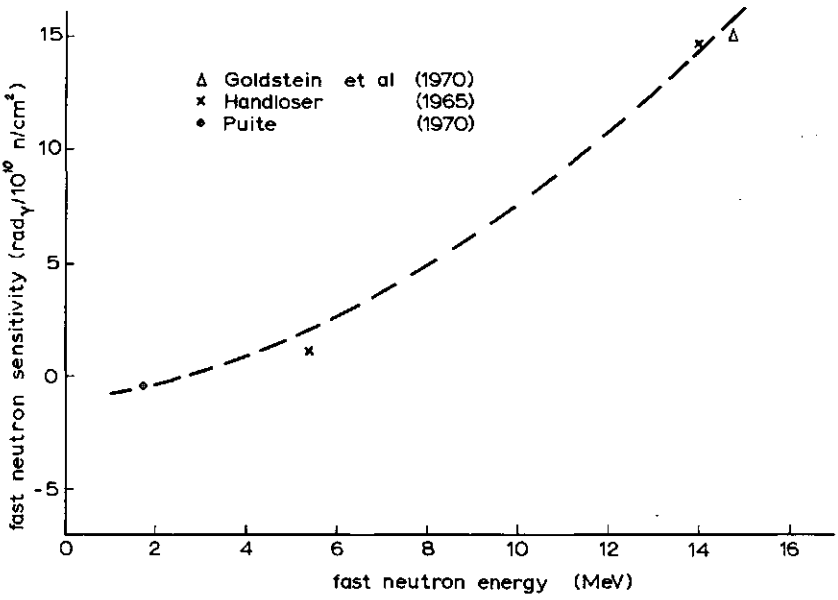

Fig.25. Reported values of fast neutron sensitivities of CaF_2:Mn for different neutron energies.

The fast neutron sensitivity of CaF_2:Mn for different energies is plotted in Figure 25. The increase in sensitivity at higher neutron energies can be ascribed to the increase in ionization relative to the loss of electrons in P traps, produced during displacements.

Conclusion

CaF_2 thermoluminescent powder can be used for measuring the gamma component of a mixed thermal neutron - gamma field. The thermal neutron sensitivity is small compared to sensitivities reported for other phosphors. No permanent change in TL sensitivity for gamma rays has been found after irradiation in a thermal neutron field for fluences up to 4×10^{12} n/cm^2.

The fast neutron experiments showed that a pre-exposure to gamma rays followed by a fast neutron irradiation does not result in a loss of TL response. Also no change in gamma ray TL sensitivity was observed when the powder was first exposed to fast neutrons up to fluences of 8×10^{13} n/cm^2, read out and then exposed to gamma rays. The fast neutron sensitivity is made up of a positive ionization component which is strongly dependent on neutron energy and a negative component arising from the formation of traps, which is less energy dependent. Thus, the sensitivity may be negative for low neutron energies as has been found here.

3.5 The trapping centers in CaF_2:Mn

3.5.1 The correlation between TSEE and TL in CaF_2:Mn determined by the simultaneous measurement of both phenomena

Presented at the Third International Symposium on Exo-electrons, Braunschweig, 6-8 July, 1970.

Introduction

The simple thermoluminescent (TL) glow curve of CaF_2:Mn, a generally used thermoluminescent powder, does in fact consist of several unresolved glow peaks due to different types of trapping centers (Figure 26). This composite character of the glow curve has been shown previously by

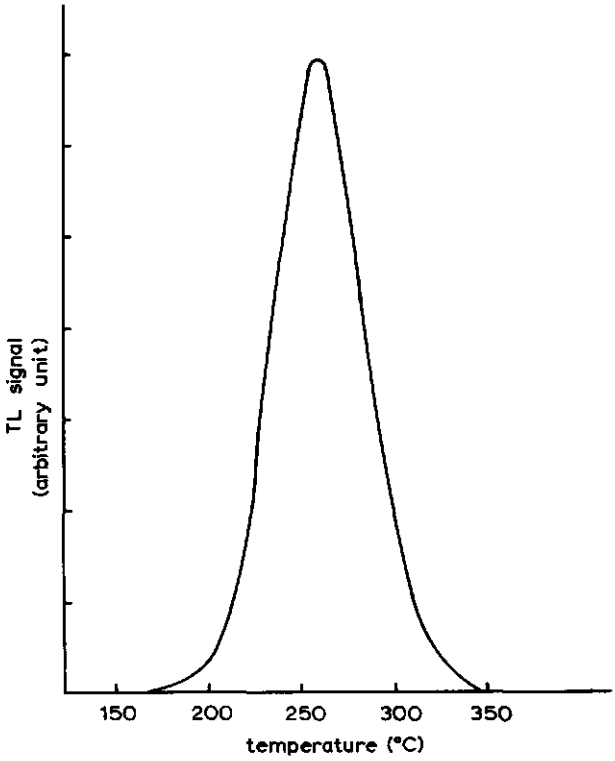

Fig.26. TL glow curve of CaF_2: 3 mole % Mn (Philips) using a heating rate of 24°C/min.

Schulman et al.(1969) with a post-exposure annealing of his CaF_2:Mn (Naval Research Laboratory, USA), while UV exposure of already read out CaF_2:Mn from Philips (the Netherlands) (Puite, 1968) has also given evidence for the complex character of the glow curve.

In an attempt to obtain information about the origin of the unresolved peaks simultaneous measurements of TL and TSEE on CaF_2: 3 mole % Mn (Philips) have been carried out. Special precautions have been taken to prevent the light produced by the gas discharge during the TSEE measurements from interfering with the TL signal. Also attention has been paid to a correct temperature assessment.

The TL and TSEE data obtained have been compared with TL data from undoped CaF_2 and CaF_2: 0.1 mole % Mn. Also optical density (OD) measurements on single crystals of these samples and on single crystals of CaF_2: 2 mole % Mn have been carried out. These combined measurements have resulted in some insight in the type of trapping centers, which are responsible for the TL and TSEE signals of CaF_2:Mn.

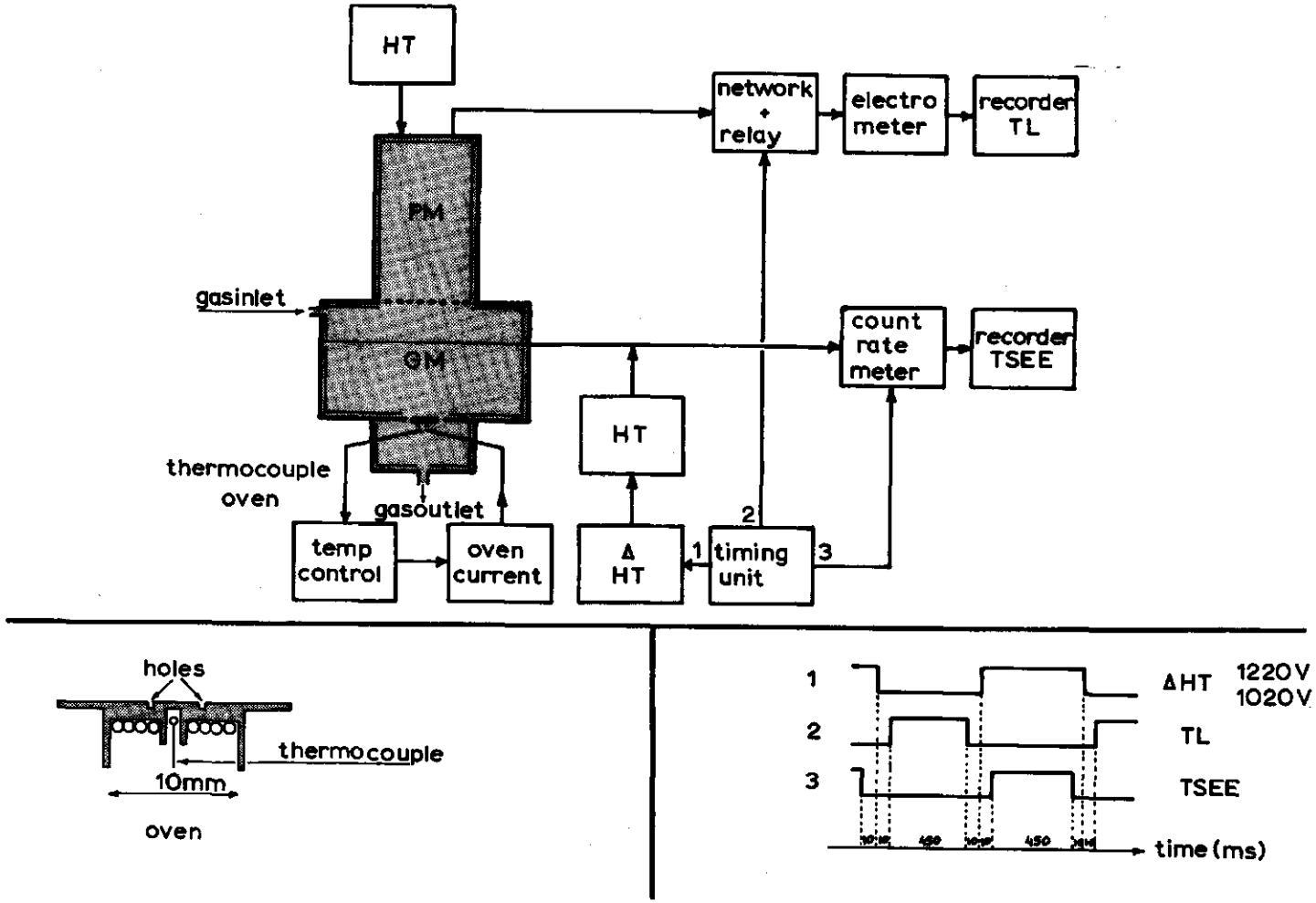

Fig.27. Apparatus for simultaneous measurement of TL and TSEE.

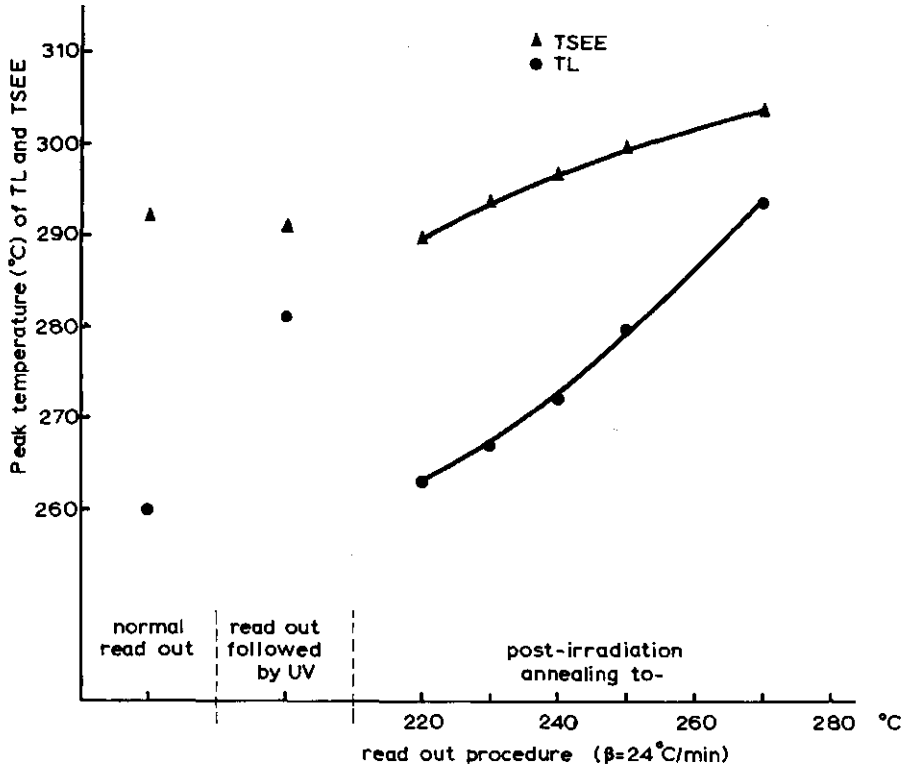

Fig.28. TL and TSEE peak temperatures for CaF_2: 3 mole % Mn (Philips) using different read out procedures.

Methods

The apparatus for measuring the TL and TSEE signals simultaneously is shown in Figure 27. The gamma irradiated powder was heated in three small holes which have a diameter of 0.9 mm each. A constant heating rate of 24°C/min was used with a thermocouple situated at a distance of 3 mm from the holes. The temperature at the position of the powder and the influence of the gas flow on the temperature at this position was determined with a second thermocouple in one of the holes. The temperature difference between the positions of the thermocouples was considerable e.g. at 250°C a difference of 15°C was measured both with and without a gas flow. A mixture of helium gas (98.7 %) and isobutane (1.3 %) was flowed through the counter, which was used in the GM region. A useful plateau could be obtained up to an oven temperature of 500°C.

The TL signal was detected with a photomultiplier on top of the counter. Because the TL from CaF_2:Mn is emitted at 500 nm, an optical

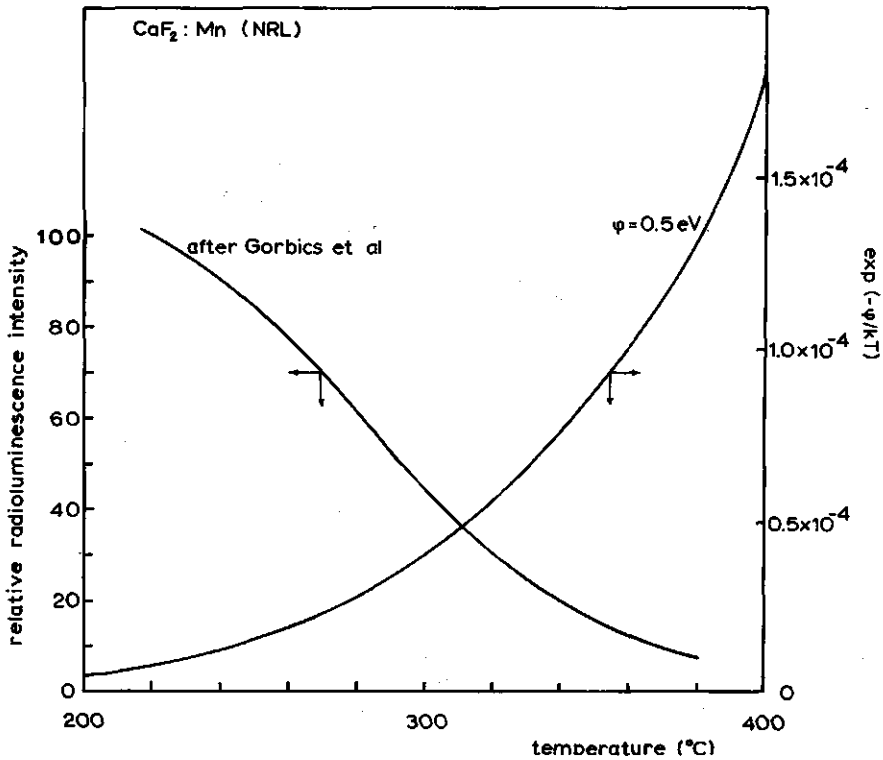

Fig.29. Effects influencing the positions of the TL and TSEE peaks of CaF_2:Mn.

filter was used which only transmitted the spectral region of 485 - 515 nm. The TL signal proved to be distorted by the light arising from the gas discharges in the counter. To avoid this a chopper system has been used in order to decrease the high tension on the wire periodically by 200 V to stop the discharges. During this period, being 450 msec, only the TL signal was recorded. When the GM counter had reached its working potential of 1220 V again only the TSEE signal was recorded, also over a period of 450 msec (see also Figure 27).

Results and Conclusion

The peak temperatures of TL and TSEE for different read out procedures are shown in Figure 28, e.g. the results of a post-irradiation annealing of CaF_2:Mn (Philips), where the powder was linearly heated up to different temperatures. Due to the composite character of the TL glow curve a shift of the TL peak to a higher temperature is found when the maximum annealing temperature is increased. Apparently, the position of

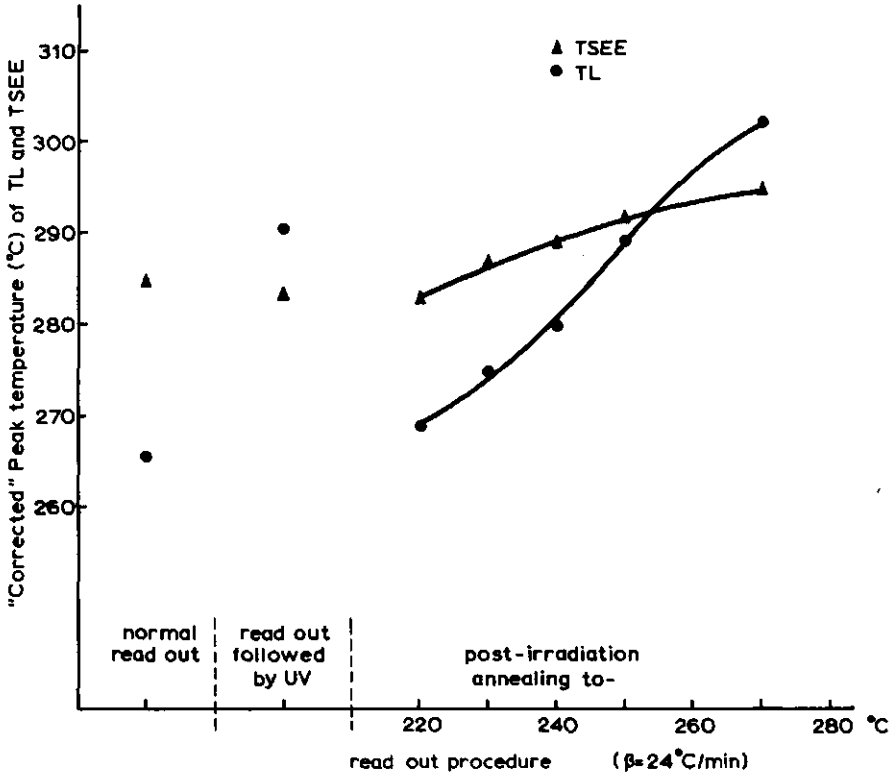

Fig.30. 'Corrected' TL and TSEE peak temperatures for CaF_2: 3 mole % Mn (Philips) using different read out procedures.

the TSEE maximum is less influenced by this annealing. The difference between the TL and TSEE maxima seems to be at minimum $\sim 10^{o}C$.

In the same Figure the difference between the TL and TSEE maxima, being also $\sim 10^{o}C$, is given when the gamma irradiated powder was first completely read out and afterwards exposed to UV light from a Philips HPLR mercury lamp. This UV transferred TL belongs to an electron trapping center.

The theory on the shift of the TL maximum relative to the TSEE maximum is complicated (Nosenko and Yaskolko, 1963). Although no direct relationship has been derived the following two effects play an important role:

a. a decrease of the luminescence intensity at higher temperatures, due to the increase in the number of non-radiative transitions compared to the number of radiative transitions. For CaF_2:Mn this so-called thermal quenching effect has been measured by Gorbics et al. (1969a).

b. the influence of the effective work function φ on the position of the

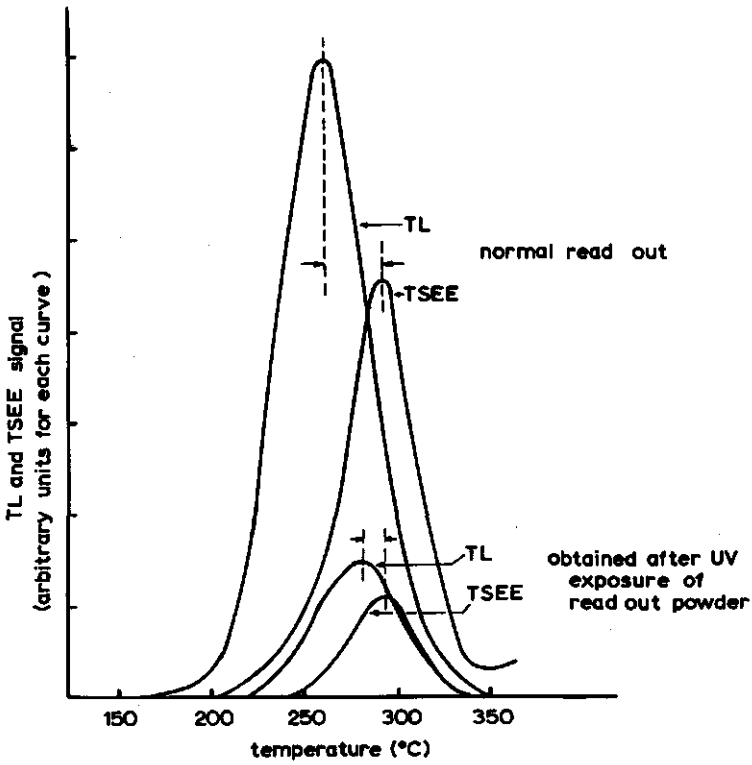

Fig.31. Shift of the positions of the TL and TSEE peaks after UV exposure of read out CaF_2: 3 mole % Mn (Philips).

TSEE maximum. A value φ of 0.5 eV was chosen for CaF_2 because Bohun and Dolejsi (1959) have reported that the best fit between the theoretical and experimental TSEE curves of CaF_2 could be obtained when the value of 0.5 eV was used.

The thermal quenching effect and the influence of the work function are shown in Figure 29. The TL glow curves have been 'corrected' for this temperature quenching while the TSEE curves have also been 'corrected' by dividing this signal by the factor exp $(-\varphi/kT)$. The resulting maxima are collected in Figure 30 and show that the temperature difference between the positions of the TL and TSEE maxima disappears when an increasing post-irradiation annealing temperature is used or when the powder is exposed to UV after being read out. It should be noted that the estimated accuracy of this temperature difference is $\pm$ 7°C. Therefore, these experiments indicate that only a part of the different types of trapping centers which contribute to the normal TL glow curve also contribute to the TSEE curve, while the remaining part of these

	origin of CaF_2	gamma dose in Mrad	optical absorption (nm)									
				Y^{++}				Y^{++}	F	Y^{++}		Y^{++}
O'Connor and Chen (1963)	Harshaw with 5×10^{-4} % Y	5		580				400		335		225
present work	Vinor (Y free)	5.7							377			
	M R C	5.7		580				406		328		228
	Semi-Elements (0.1 % Mn)	5.7	700	580			420					
	M R C (2 % Mn)	0.1 5			567 563	435	420			320	304	

Table 10. Color centers in CaF_2:Mn.

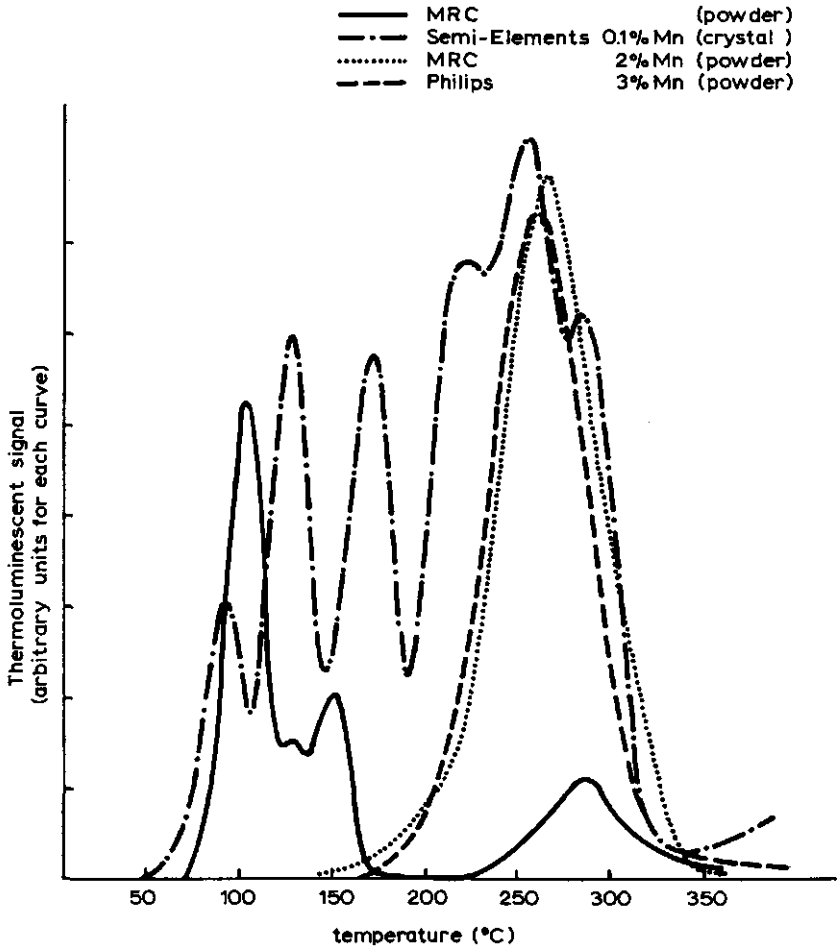

Fig.32. TL glow curves of CaF_2 samples.

centers are probably hole centers.

Figure 31 illustrates the difference between the peak temperatures of the TL and TSEE curves for a normal read out and for a read out after UV exposure.

The results of optical density (OD) measurements on gamma irradiated single crystals of CaF_2, some of which are doped with manganese, are shown in Table 10. These experiments were carried out at room temperature with a Unicam SP 700 recording spectrophotometer. Very pure CaF_2 can hardly be colored by irradiation at room temperature. O'Connor and Chen (1963) have demonstrated that an absorption at very high doses can often be ascribed to the contaminant yttrium Y^{3+}, which has the same ionic radius as Ca^{++}. From our samples the CaF_2 of Materials Research Corporation (MRC) and the CaF_2: 0.1 mole % Mn both show the presence of yttrium, while in the crystals doped with ~ 2 mole % of Mn the yttrium absorption is obviously influenced by the presence of Mn.

The Vinor crystal, which is yttrium free, shows F-center absorption due to the presence of vacancies introduced by oxygen.

Figure 32 shows the TL of these samples together with the normal glow curve of the CaF_2 from Philips. The undoped CaF_2 from MRC, which exhibits Y^{++} absorption bands, has only one high temperature TL peak at

CaF_2 powders			F			Y^{++} Mn^{++}	Y^{++}	tribo	gamma dose
Vinor			149		250			340	5 Mrad
M R C	100	127	149				292		6 krad
Semi-Elements 0.1 % Mn		123	169	211		262	300		6 krad
M R C ~2% Mn				265					6krad
Philips # 5 ~3% Mn				260					6 krad
idem, with UV exposure after read out						281			30krad

Table 11. TL maxima of CaF_2 and CaF_2:Mn in ^{o}C. For the Philips powder the position of TSEE is shaded.

292°C. The CaF_2 doped with 0.1 mole % Mn from Semi-Elements, which exhibits yttrium absorption at 580 nm, has TL peaks at 262°C and 300°C. In the CaF_2 doped with 2 mole % Mn from MRC, which also contains yttrium, only one broad peak is found with a maximum at 265°C; in the normal TL powder from Philips with 3 mole % Mn the maximum occurs at 260°C. The average positions of the TL maxima of these materials are shown in Table 11.

If the knowledge of the various CaF_2 samples studied is combined, taking into account: the chemical analysis (Table 2 of section 2.1.2), the OD measurements, and the TL measurements, the following conclusions may be drawn,

a. the TL occurring at 290 to 300°C can be ascribed to an Y^{++} centre and the TL occurring at 260°C is probably associated with an $Y^{++} + Mn^{++}$ complex.

b. the TSEE, which peaks at 292°C, the UV transferred TL, which peaks at 281°C and the high temperature components of the composite TL peak in the Philips powder are associated with the Y^{++} and probably $Y^{++} + Mn^{++}$ centers.

c. other divalent rare earth ions such as Ho^{++}, Sm^{++} and Tm^{++} might be present instead of Y^{++} ions.

3.5.2 TSEE experiments with CaF_2 powder and single crystals of CaF_2, undoped and doped with manganese

Introduction

In the preceeding section 3.5.1 it was shown that yttrium centers are present and yttrium + manganese centers may be present in irradiated CaF_2:Mn (Philips) powder. From post-irradiation annealing experiments with this powder it was concluded that only a part of the different types of trapping centers which contribute to the normal TL glow curve also contribute to the TSEE curve, whilst the remaining centers are probably hole centers.

It is not clear where these holes are trapped, although Schulman (1967) has mentioned the Mn^{++} sites as possible hole traps.

A comparison of TSEE and TL data of CaF_2 samples, undoped and doped with manganese, could contribute to a distinction between the type of centers in CaF_2:Mn.

Methods and Results

The TSEE experiments have been carried out with the apparatus described in detail in section 2.2.2. A strictly linear heating rate of 24°C/min was used. The shape of the TSEE curve and the position of the peak maximum T_m of the various samples as compared to the corresponding TL data were of main interest.

Apart from these measurements a dose response curve for one of the samples (CaF_2:Mn from Philips) has been recorded. The TSEE signal obeyed the emperical equation,

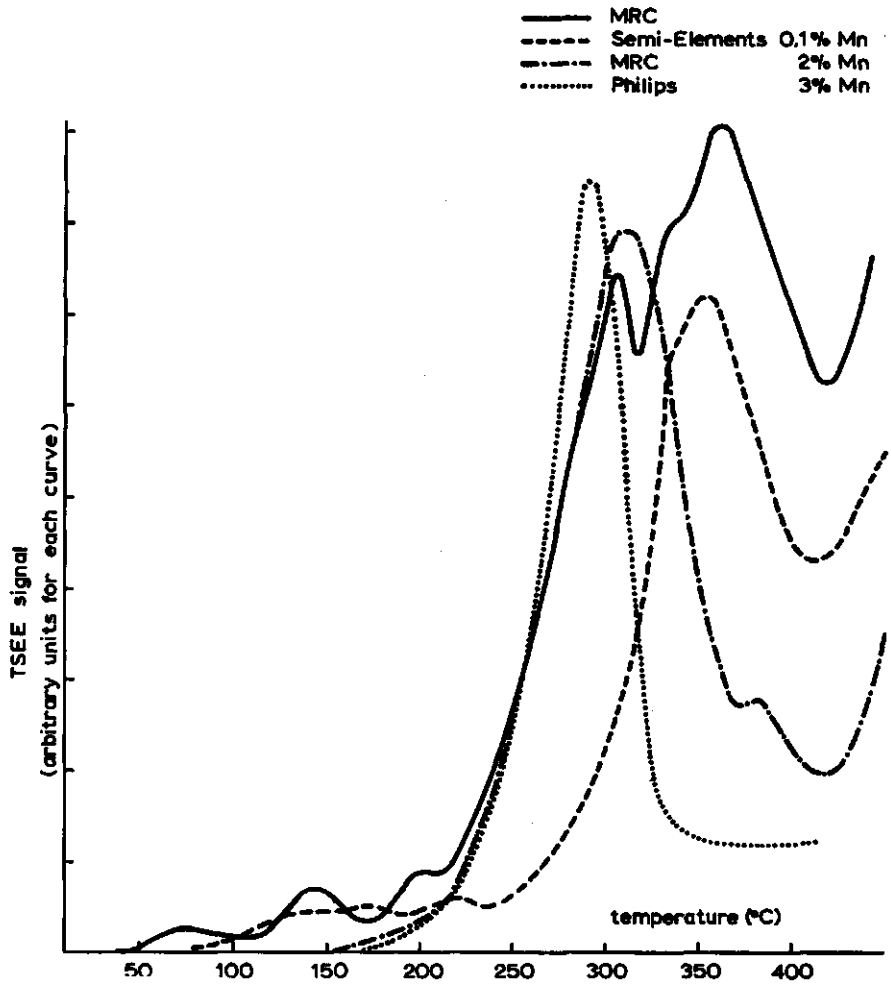

Fig.33. TSEE curves of CaF_2 samples.

$$\text{TSEE signal} = a\ D^p \qquad [25]$$

where a is a constant and p = 0.76 for a gamma dose D between 0.5 - 30 krad.

This non-linearity with dose has been found by many authors (Becker, 1970; Kramer, 1968). It is due to a charging of the sample surface and can be avoided by mixing the powder with graphite (Kramer, 1966).

Some typical TSEE curves are shown in Figure 33. The peak maxima of the CaF_2 samples (crystals and powders) are listed in Table 12, in which the position of the TL maxima is also given. The TL glow curves have been recorded using a photomultiplier on top of the TSEE counter as described in section 3.5.1.

Discussion and Conclusion

Comparing the two MRC samples and the sample of Semi-Elements it is clear that the 310°C TSEE peak is due to the Y^{++} center. The TL maximum for this center was found at ~ 300°C. Using equations 4 and 3 of section 1.2 a trap depth of 1.0 ± 0.2 eV (estimated error) along with a frequency factor of 9 x 10^6/sec is obtained for the Y^{++} center in the undoped MRC sample. Substituting these E and s values in equation 7 of section 1.4 an E + φ value of 0.9 ± 0.2 eV (estimated error) is calculated. Within the limits of accuracy of the estimation of E and s, this would imply that φ << E. Therefore, the value of φ is probably ~ 0 - 0.1 eV.

When a value of φ = 0 eV had been used in section 3.5.1 instead of 0.5 eV the temperature difference between the TL and TSEE maxima recorded would have been negligible after both UV exposure of read out CaF_2 (Philips) and post-irradiation annealing to 270°C. This indicates that the value of φ = 0.5 eV is overestimated.

The Mn^{++} ions are situated at Ca^{++} ion lattice positions (see section 1.5) and have an energy level of some eV above the valence band. The exact position of this level is not known. It is well known that the Mn^{++} ions can easily be converted into Mn^{3+} ions by trapping one hole. The TL peak at 259°C occurring in CaF_2: 0.1 mole % Mn is probably due to these hole traps because no TSEE peak was observed in the neighbourhood of this temperature for gamma doses < 12 krad. At high gamma doses

sample \ center	D_γ krad				F					$(Y_{Mn}$		Y^{++}				
			e^-	h^+	e^-				e^-	$h^+(e^-)$		e^-				
MRC	6	TSEE	99			161	174	213				310	340	363	381	398
7.6 ppm Y	6	TL	106	133		161						301				370
Semi-Elements	6	TSEE	108		153	169		206		263*	294*	312	328	355		395
0.1% Mn 8.3 ppm Y	6	TL	90	124		170		213		259		298				
MRC	6	TSEE										311				
~2% Mn	6	TL								267						
Philips	6	TSEE									292					
~3% Mn 0.03 ppm Y	6	TL								260						
idem, with post-irr. annealing to 270°C	6	TSEE									303					
	6	TL									294					
Vinor	5000	TSEE				175			263		309		343		379	390
no Y	5000	TL	104		148				250				323		340	
Harshaw	5000	TSEE			152	168					304				371	
0.17 ppm Y	5000	TL				160					279				333	

* D_γ = 5000 krad

heating rate 24 °C/min

Table 12. TSEE and TL maxima of CaF_2 samples. The main peaks are underlined.

(5 Mrad), however, a TSEE peak has been observed at 263°C indicating that electrons may also be released in this temperature region. This effect occurs only incidently and was found only twice in eight measurements.

After irradiation of CaF_2: 3 mole % Mn (Philips) powder both Y^{++} and Mn^{3+} centers are expected to occur. Other rare earth centers such as Ho^{++}, Sm^{++} and Tm^{++}, all trapped electron centers, could also be present. As the manganese concentration is six orders of magnitude greater than the concentration of yttrium impurities (0.03 ppm) the manganese centers will be dominant. Both the TL and TSEE maxima are shifted to lower temperatures, compared to the MRC samples doped with 2 mole % Mn, which have a high contamination of 7.6 ppm of yttrium (see Table 2 of section 2.1.2).

Furthermore Table 12 indicates the presence of F-centers already demonstrated in Vinor crystals with optical absorption measurements (section 3.5.1). Therefore, F-center type traps may be present in the temperature region of 150 - 170°C.

3.6 Thermoluminescence of collagen

Introduction

The radiation induced phenomena in collagen, a protein present in skin, tendons, bones and teeth, are only partly understood. The following types of damage have been reported after irradiation of dry collagen (Bailey, 1967; Bailey, 1968b),

a. peptide chain scission. This will lead to an increased solubility and to reduction in the shrinkage temperature. A decrease in this temperature is considered, however, to be mainly due to a disorganization of the secondary structure and depend primarily on b.

b. breakage of the intramolecular hydrogen bonds that hold the three peptide chains together.

c. interchain cross-links. This effect is dependent on the presence of water and is probably due to the abstraction of an H atom from the molecule by the OH radical from the water and interaction of the two molecular radicals.

Electron spin resonance (ESR) studies on irradiated collagen have shown that at room temperature the radicals are localized at certain specific sites (Zimmer and Muller, 1965). The ESR signal revealed a

composite pattern of the glycine and alanine radical and no components characteristic of proline and hypoproline. However, the abundance of these four amino acids in collagen is about 33, 11, 12 and 9 residues/ 100 residues, respectively (Veis, 1964). A physical process of exciton migration or an excitation of collective electronic levels has been suggested to explain ESR data (ten Bosch, 1967).

Apart from ESR measurements thermoluminescence studies may give valuable information on the radiation effects in collagen (see section 1.6 of this thesis).

Materials and Methods

Dry collagen (ex bovine tendon) was purchased from Koch-Light Ltd., Colnbrook, England, and irradiated at liquid nitrogen temperature in a brass sample holder. This sample holder was closed by a diaphragm during irradiation and transport to avoid light effects on the sample and a warming up of the sample surface. A Philips deep therapy X-ray unit (250 kVp, HVL 1.5 mm Cu) was used and a dose rate of 0.5 krad/min was obtained. The TL signal was recorded over the temperature range of 77 - 273°K, by heating the sample at a linear rate of 13°K/min. The time between the end of the irradiation and the beginning of the measurement was normally 10-15 minutes.

Results and Discussion

The glow curve of collagen (Figure 34) shows three distinct maxima at 138, 210 and 256°K. Water, which has a glow peak at 165°K, does not contribute. Initial rise calculations (equation 4 of chapter 1.2) for the dominant peak at 210°K resulted in a trap depth E of 0.35 eV.

Comparing these data with the TL data reported by Augenstine et al. (1960) (see also Table 1 of chapter 1.6) for all the constituent amino acids of collagen it follows that none of the traps present in these amino acids is found at ~ 210°K with a trap depth of 0.3-0.4 eV. An explanation may be that the charge distribution of the amino acids, which could lead to the observed trap properties, is modified in the collagen resulting in different trapping sites. This suggestion has also been forwarded by Augenstine et al. (1961) in relation to other proteins. Another explanation may be that traps are located near peptide links or

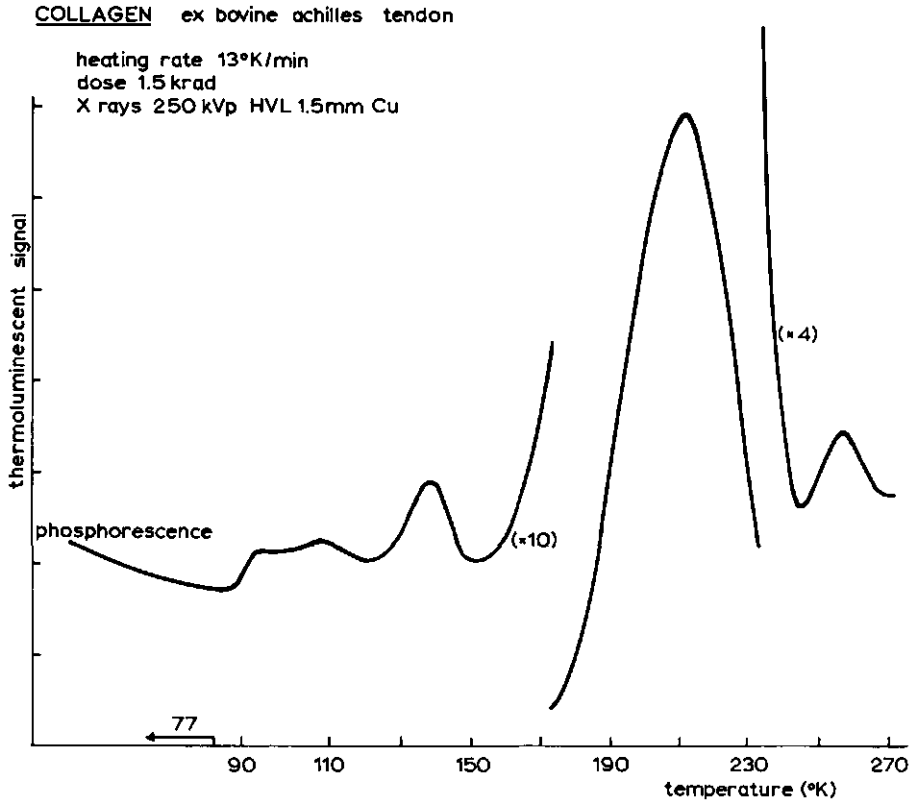

Fig.34. Thermoluminescent glow curve of collagen (from Koch-Light, Ltd.) in the temperature range of 77 - 273°K.

that the helix structure is of importance for electron trapping.

In general, extremely high doses (10^3 - 10^7 rad) are required to produce detectable effects on dried samples of collagen (Bailey et al., 1962; Cooper and Russell, 1969). With thermoluminescence, however, doses of 25 rad already result in a distinct TL response.

Further measurements will be directed to an investigation of the trapping sites and the relation between thermoluminescence and biological damage.

Summary

Thermoluminescent phenomena in CaF_2 powder doped with 3-4 mole % manganese and having dimensions of 10-15 μm have been studied. The material was prepared for dosimetric purposes at the Philips laboratories, Eindhoven, the Netherlands.

The gamma irradiated powder showed a single glow peak at 260°C when the powder was heated at a constant heating rate of 24°C/min. This glow curve in fact consisted of several unresolved peaks due to different types of trapping centers. Normally, all these traps are emptied during one heating cycle. However, UV exposure of already read out CaF_2 gave rise to a second reading indicating a filling of the dosimetry traps from deeper levels. Thermally stimulated exo-electron emission and thermoluminescence measurements using CaF_2 samples doped with 0.1 mole % and 2 mole % manganese and undoped samples have led to the conclusion that both electron- and hole traps are present in the CaF_2:Mn (Philips); Y^{3+} and other trivalent rare earth ions, being the electron traps and Mn^{++} centers, being the hole traps.

The thermoluminescent sensitivity of CaF_2 for alpha particles and protons compared to gamma rays was investigated. CaF_2 powder, surrounded by boron and nitrogen containing liquids, has been irradiated in a thermal neutron field. The $^{10}B(n,\alpha)^{7}Li$ and $^{14}N(n,p)^{14}C$ reactions occurring in the liquids gave rise to an extra response in the CaF_2 due to the alpha particles and protons. Powder surrounded by alcohol and irradiated in a fast neutron field gave an extra response due to the proton recoils produced in the alcohol. The response from these charged particles relative to that of gamma rays was found to be 3, 5 and 11 %, respectively, based on absorbed dose in the liquid. Also the thermoluminescent sensitivity for the thermal and fast neutrons themselves has been investigated. For thermal neutrons a value of 0.07 rad per 10^{10} n/cm^2 was found, whilst the fast neutron 'sensitivity' proved to be -0.43 rad per 10^{10} n/cm^2 for a neutron spectrum, having an average energy of 1.7 MeV. In order to explain this negative value a model has been

developed assuming that the 'sensitivity' is made up of a positive ionization component which is strongly dependent on energy and a negative component arising from the formation of deep traps, which is less energy dependent.

Biological molecules often show thermoluminescent phenomena when they are irradiated at liquid nitrogen temperature. Preliminary experiments have been carried out with the protein collagen. Even at doses of 25 rad a distinct TL glow curve has been obtained.

References

Almond, P.R., K. McGray, D. Espejo and S. Watanabe — 1968 Proc. Sec. Int. Conf. on Luminescence Dosimetry, p. 411, Gatlinburg

Arends, J. — 1964 Phys. stat. sol. 7, 805

Aten, Jr, A.H.W. — 1966 Document submitted to the Euratom Working Group on Reactor Dosimetry

Augenstine, L.G., J.G. Carter, D.R. Nelson, H.P. Yockey — 1960 Radiation Res. Suppl. 2, 19

Augenstine, L.G., J.G. Carter, D.R. Nelson and H.P. Yockey — 1961 in: Free radicals in Biological Systems, p. 149, Academic Press, New York

Auxier, J.A., K. Becker and E.M. Robinson (eds.) — 1968 Proc. Sec. Int. Conf. on Luminescence Dosimetry, Gatlinburg

Ayyangar, K., A.R. Reddy and G.L. Brownell — 1968 Proc. Sec. Int. Conf. on Luminescence Dosimetry, p. 525, Gatlinburg

Bailey, A.J., J.R. Bendall and D.N. Rhodes — 1962 Int. J. appl. Radiat. Isotopes 13, 131

Bailey, A.J. — 1967 Radiation Res. 31, 206

Bailey, A.J. — 1968 a, in: Comprehensive Biochemistry, vol. 26B

Bailey, A.J. — 1968 b, in: Int. Rev. Connect. Tissue Res. vol. 4, p. 233

Baker, J.M., B. Bleaney, F.R.S. and W. Hayes — 1958 Proc. Roy. Soc. London, A 247, 141

Becker, K. — 1970 Atomic Energy Rev. 8, 173

Bewley, D.K. — 1969 Private communication

Billington, D.S. and J.H. Crawford — 1961 Radiation Damage in Solids, Ch. 2, Princeton University Press

Bogaardt, M., J. Coehoorn, W. Hofman, and W.W. Nijs — 1964 Proc. Third Conf. Peaceful Use of Atomic Energy 7, 187

Bohun, A. — 1955 Czech. J. Phys. 5, 224

Bohun, A. and J. Dolejsi — 1959 Czech. J. Phys. 9, 578

Bohun, A. 1963 Phys. stat. sol. 3, 779

Bosch, J.J. ten 1967 thesis, University of Utrecht, the Netherlands

Brooke, L. and R. Schayes 1967 in: Solid state and chemical radiation dosimetry in medicine and biology, p 31, IAEA, Vienna

Carter, J.G., D.R. Nelson and L.G. Augenstein 1963 Appl. Phys. Lett. 2, 226

Cervigni, T., C. Bassanelli, G. Caserta, R.F. Laitano 1969 Radiation Res. 38, 579

Chadwick, K.H. and W.F. Oosterheert 1969 Atompraxis 3, 178

Chadwick, K.H., H.P. Leenhouts, W.F. Oosterheert and K.J. Puite 1969 Paper presented at the IAEA panel on Neutron irradiation of seeds, Knoxville, USA

Cooper, D.R. and A.E. Russell 1969 Biochem. J. 113, 263

Cristensen, P. 1968 Proc. Sec. Int. Conf. on Luminescence Dosimetry, p. 91, Gatlinburg

Daniels, F. 1950 Techn. Comm. Army Chem. Center Maryland, part I, p. 148

Dieck, L. 1966 Report JUL-355-RX, Jülich, Germany

Dolejsi, J., J. Kanturek, A. Bohun, J. Trnka 1958 Czech. J. Phys. 8, 548

Endres, G.W.R. and L.F. Kocher 1968 Proc. Sec. Int. Conf. on Luminescence Dosimetry, p. 486, Gatlinburg

Fleming, R.J. and R.M. Kerr 1965 Nature 208, 1198

Fong, F.K. and P.N. Yocom 1964 J. Chem. Phys. 41, 1383

Fowler, J.F. and F.H. Attix 1966 in: Radiation Dosimetry II, Ch. 13, Academic Press, New York

Ginther, R.J. and R.G. Kirk 1956 U.S. Naval Research Laboratory, Report of Progress, p 12

Ginther, R.J. and D. Kirk 1957 J. Electrochem. Soc. 104, 365.

Goldstein, N., W.G. Miller and P.F. Rago 1970 Health Phys. 18, 157

Gorbics, S.G., F.H. Attix and J.A. Pfaff 1967 Int. J. appl. Radiat. Isotopes 18, 625

Gorbics, S.G., A.E. Nash and F.H. Attix 1969 a, Int. J. appl. Radiat. Isotopes 20, 829

Gorbics, S.G., A.E. Nash and F.H. Attix 1969 b, Int. J. appl. Radiat. Isotopes 20, 843

Görlich, P., H. Karras, A. Köthe and K. Kühne 1961 Phys. stat. sol. 1, 366

Görlich, P., H. Karras, Ch. Symanowski and P. Ullmann 1968 Phys. stat. sol. 25, 93

Gouverneur, F.C.M. and K.J. Puite 1970 Internal Report no. 94, ITAL, Wageningen, the Netherlands

Handloser, J.S. 1965 Personnel Dosimetry for Radiation Accidents, p. 115, IAEA, Vienna

Harrington, W.F. and P.H. von Hippel 1961 in: Advances in protein chemistry, p. 1, Academic Press, New York

Hart, E.J. and R.L. Platzman 1956 in: Mechanisms in Radiobiology, vol. I, p. 93, Academic Press, New York

Hartog, H.W. den 1969 thesis, University of Groningen, the Netherlands

Holm, N.W., A. Brynjolfsson and J.E. Maul 1961 in: Selected Topics in Radiation Dosimetry, p. 371, IAEA, Vienna

Holzapfel, G. 1969 Phys. stat. sol. 33, 235

Hughes, D.J. 1953 Pile Neutron Research, Addison-Wesley Publishing Co.

IAEA 1967 Neutron irradiation of seeds, Technical Report Series no. 76, p. 74, IAEA, Vienna

Kamikawa, T., Y. Kazumata, A. Kikuchi and K. Ozawa 1966 Phys. Letters 21, 126

Kanturek, J. 1956 Czech. J. Phys. 6, 4

Karzmark, C.J., J. White and J.F. Fowler 1964 Phys. Med. Biol. 9, 273

Kastner, J., B.G. Oltman, P. Tedeschi and K.F. Eckerman 1969 Proc. 14th Annual Meeting Health Phys. Soc., Pittsburgh

Kramer, J. 1949 Z. Phys. 125, 739

Kramer, J. 1951 Z. Phys. 129, 34

Kramer, J. 1966 Z. angew. Phys. 20, 411

Kramer, J. 1967 Z. angew. Phys. 22, 272

Kramer, J. 1968 Proc. Sec. Int. Conf. on Luminescence Dosimetry, p. 180, Gatlinburg

Law, J. 1970 Phys. Med. Biol. 15, 301

Lehman, R.L. and R. Wallace 1964 in: Electronic Aspects of Biochemistry, p. 43, Academic Press, New York

Lin, F.M. and J.R. Cameron 1968 Health Phys. 14, 495

Marrone, M.J. and F.H. Attix 1964 Health Phys. 10, 431

Mason, E.W. 1970 Phys. Med. Biol. 15, 79

McGlynn, S.P., F.J. Smith and G. Cilento 1964 Photochem. Photobiol. 3, 269

Nosenko, B.M. and V.Ya. Yaskolko 1963 Opt. i. Spektr. Suppl. 1, 117

Nummedal, D. and H.B. Steen 1969 Radiation Res. 39, 241

O'Connor, J.R. and J.H. Chen 1963 Phys. Rev. 130, 1790

Oltman, B.G., J. Kastner, P. Tedeschi and J.N. Beggs 1967 Health Phys. 13, 918

Patel, A.R. and C.C. Desai 1965 Z. Kristallogr. 121, 431

Patel, A.R. and C.C. Desai 1968 Z. Kristallogr. 126, 199

Puite, K.J. and J.G. de Swart 1965 Internal Report no. 60, ITAL, Wageningen, the Netherlands

Puite, K.J. 1968 Int. J. appl. Radiat. Isotopes 19, 397

Puite, K.J. 1969 Health Phys. 17, 661

Ramachandran, G.N. 1963 in: Aspects of Protein Structure, G.N. Ramachandran ed., Academic Press, New York

Randall, J.T. and and M.H.F. Wilkins 1945 Proc. Roy. Soc. London 184, 366

Reddy, A.R., K. Ayyangar and G.L. Brownell 1969 Radiation Res. 40, 552

Rich, A. and F.H.C. Crick 1961 J. Mol. Biol. 3, 483

Schayes, R., C. Brooke, I. Kozlowitz and M. Lheureux 1967 in: Luminescence Dosimetry, p 138, US AEC

Schulman, J.H. and E.J. West 1963 Rev. scient. Instrum. 34, 863

Schulman, J.H. 1967 in: Solid state and chemical radiation dosimetry in medicine and biology, p. 3, IAEA, Vienna

Schulman, J.H., R.J. Ginther, S.G. Gorbics, A.E. Nash, E.J. West, F.H. Attix — 1969 Int. J. appl. Radiat. Isotopes 20, 523

Singh, B.B. and A. Charlesby — 1965 Int. J. Rad. Biol. 9, 157

Spurny, Z. — 1969 Health Phys. 17, 349

Steen, H.B. — 1968 Scand. J. clin. Lab. Invest. Suppl. 106, 21

Sujak, B. and K. Gieroszynska — 1967 Acta phys. pol. 32, 541

Tochilin, E., N. Goldstein and W.G. Miller — 1969 Health Phys. 16, 1

Unruh, C.M., W.V. Baumgartner, L.F. Kocher, L.W. Brackenbush and C.W.R. Endres — 1967 Neutron Monitoring, p. 433, IAEA, Vienna

Veis, A. — 1964 The Macromolecular Chemistry of Gelatin, Academic Press, New York

Wallace, R.H. and P.L. Ziemer — 1968 Proc. Sec. Int. Conf. on Luminescence Dosimetry, p. 140, Gatlinburg

Weinberg, C.J., D.R. Nelson, J.G. Carter, L.G. Augenstine — 1962 J. Chem. Phys. 36, 2869

Welling, L. and S. Bakerman — 1964 Nature 201, 495

Wingate, C.L., E. Tochilin and N. Goldstein — 1965 US NRDL-tr-909

Woodley, R.G. and N.M. Johnson — 1967 Luminescence Dosimetry, p. 502, US AEC

Zanelli, G.D. — 1968 Phys. Med. Biol. 13, 393

Zijp, W.L. — 1965 RCN Report no. 37, Petten, the Netherlands

Zimmer, K.G. and A. Muller — 1965 in: Current Topics in Radiation Research, M. Ebert and A. Howard eds., vol. 1, p.1, North-Holland Publ., Amsterdam

Aan de velen die hebben bijgedragen aan dit proefschrift ben ik zeer veel dank verschuldigd. De bekwame technische assistentie van de heer D.L.J.M. Crebolder heeft een groot deel van de experimenten mogelijk gemaakt. De discussies met de hoogleraren J. Arends en A.J. Dekker en de collega's W.F. Oosterheert, K.H. Chadwick en H.P. Leenhouts zijn mij tot grote hulp geweest, evenals de bezielende steun van de heer D. de Zeeuw.

Met vele werkers van het ITAL, de onderzoekers, de Radiobiofysika- en dosimetriegroep, de reactorbedieningsgroep, de mensen van de werkplaats, de typekamer (met name de heer H. Boersma) en de bibliotheek heb ik veelvuldige kontakten gehad. Deze en de plezierige werksfeer op het ITAL heb ik zeer gewaardeerd.